

**KERNFORSCHUNGSZENTRUM  
KARLSRUHE**

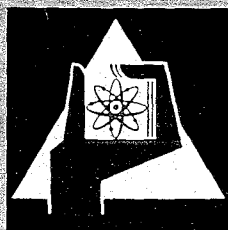
Oktober 1967

KFK 637  
SM 101/18  
EUR 3681 e

Institut für Reaktorbauelemente

Parametric Study of the Dynamic Behaviour and Stability of a  
Steam-Cooled Fast Reactor with an Integrated Coolant Cycle

F. Erbacher, W. Frisch, W. Hübschmann, S. Malang, L. Ritz, G. Woite



GESELLSCHAFT FÜR KERNFORSCHUNG M. B. H.

KARLSRUHE



KERNFORSCHUNGSZENTRUM KARLSRUHE

Oktober 1967

KFK 637  
SM 101/18  
EUR 3681 e

Institut für Reaktorbauelemente  
Institut für Reaktorentwicklung

PARAMETRIC STUDY OF THE DYNAMIC BEHAVIOUR AND STABILITY OF A  
STEAM-COOLED FAST REACTOR WITH AN INTEGRATED COOLING CYCLE <sup>+)</sup>

F. Erbacher, W. Frisch, W. Hübschmann,  
S. Malang, L. Ritz, G. Woite

GESELLSCHAFT FÜR KERNFORSCHUNG MBH., KARLSRUHE

<sup>+)</sup> Work performed within the association in the field of fast  
reactors between the European Atomic Energy Community and  
Gesellschaft für Kernforschung mbH., Karlsruhe



PARAMETRIC STUDY OF THE DYNAMIC BEHAVIOUR AND STABILITY OF  
A STEAM-COOLED FAST REACTOR WITH AN INTEGRATED COOLING CYCLE

ABSTRACT:

The following report shows that in a steam-cooled fast breeder reactor it is possible in principle to produce inherent stability and safety from accidents by the feedback of the cooling cycle on the core. The effects of various parameters on stability and safety are determined for these disturbances: Reactivity disturbance, blower failure, load changes, various pipe ruptures, and inadvertent fast unflooding. This results in trends and limits that should be observed in the design of the components and the arrangement of the cooling cycle. It is shown that in particular a cooling cycle integrated in a common pressure vessel produces easily inherent stability and safety of a steam-cooled fast reactor.

Table of contents

Page

1. Introduction	1
2. Inherent Stability and Inherent Safety from Accidents	2
3. Disturbances	6
3.1 Reactivity Disturbance	6
3.2 Blower Failure	8
3.3 Load Changes	11
3.4 Rupture of superheated-steam pipe	12
3.5 Rupture of saturated-steam pipe	13
3.6 Unflooding Accident	18
4. Conclusion	22

## 1. INTRODUCTION

In a steam-cooled fast reactor the coolant density coefficient is generally negative. If the average steam density in the core decreases, this implies a reactivity increase. The rate at which this reactivity increase occurs determines the extent of a possible damage caused by a failure of the safety system.

It has been shown in [1] that a compact cycle integrated in a pressure vessel is able to inherently fulfill the conditions of stability and safety from accidents to such an extent that these do not depend exclusively on the functioning of the control and safety systems. If this characteristic of inherent stability and safety from accidents is made a primary requirement, this will influence the design of the cycle and of its components.

As is shown in Fig. 1, such cycle consists of the core C, the plenum volumes for superheated and saturated steam  $V_h$  and  $V_s$ , the evaporators E, the steam blowers B, the water storage  $V_w$ , and the pipe lines connecting them. The blowers are driven by turbines  $T_b$  which are connected in series with the main power turbine  $T_p$ . The dashed line indicates that the whole cooling cycle is surrounded by a common pressure vessel.

It is the purpose of this parametric study to investigate the influence of the design and arrangement of the listed components on the stability of the cycle and its accident safety. The calculations are based on the core dimensions and the reactivity curve of the D-1 design [2].

The reported results were obtained by means of various digital codes for special problems and an analog model of the complete reactor cooling cycle [3].

## 2. INHERENT STABILITY AND INHERENT SAFETY FROM ACCIDENTS

If a reactivity increment  $\Delta k_d$  is introduced into the core, the power  $Q$  of the reactor after a short overshooting rises asymptotically to a value  $Q + \Delta Q$ . The quotient  $\frac{\Delta Q/Q}{\Delta k_d}$  is called the reactivity gain  $K_k$ . This is

$$K_k = \frac{\Delta Q/Q}{\Delta k_d} \quad (1)$$

$Q$  = reactor power

$K_k$  = reactivity gain

$\Delta k_d$  = reactivity disturbance.

If the power increment  $\Delta Q$  is not consumed by the main turbine, the increased steam generation in the evaporator will cause the pressure in the cooling cycle to rise at a rate which is inversely proportional to the energy storage capacity  $C \left[ \frac{\text{MW}_s}{\text{atm}} \right]$ .

The rise of the pressure  $p$  and the rise of the average density  $\rho$  of the steam reduce the power increment in the case of a negative steam density coefficient  $\alpha_\rho$  so that the ultimate value will be precisely the power that is taken from the main turbine. This mechanism may be utilized for the self-stabilization of reactor power in case of minor disturbances as well as for the self-control in case of changes in the power consumption.

Fig. 2a shows the time behaviour of the reactor power after a step-like reactivity increase  $\Delta k_d = 0.2 \%$  without cycle feedback. The beginning of all curves, which hold for various reactivity gains, is identical because of the prompt critical power step.

The higher the reactivity gain, the more the reactor power rises in the case of a reactivity increase. For reasons of safety and stability the reactivity gain should be as small as possible, as



is evident from Fig. 2a. The favourable influence of a low reactivity gain is obvious also from Fig. 2b, in which the feedback of the cycle has been taken into account.

The pressure increase in the cycle will start with a delay because of the various delay and dead times of the energy transport from the reactor to the water in the evaporators. These periods are combined in the delay time  $T_u$ . In case of an excessive delay time  $T_u$  the reactor power may be excited into oscillations. A buildup of these oscillations is prevented, if

$$K_k \times \alpha_g \times \frac{d\rho}{dp} \times \frac{y \times Q}{C} \times T_u < A_{crit}.$$

Here,  $y$  is the ratio of the quantity of superheated steam flowing to the evaporators to the total quantity of steam flowing through the core.

The term  $K_k \times \alpha_g \times \frac{d\rho}{dp}$  will be called pressure gain  $K_p$  below. It is negative with a negative steam density coefficient. Hence, the stability condition is

$$- K_p \times \frac{y \times Q}{C} \times T_u < A_{crit} \quad (2)$$

The value of  $A_{crit}$  depends on the composition of the delay time  $T_u$  and is a minimum of  $\frac{\pi}{2}$  under the assumption of a pure dead time and it is 4 under the assumption of two delay times of equal length.

Since there are several time constants of the same order of magnitude in this system,  $A_{crit}$  is between these limits as shown in [4].

$$\frac{\pi}{2} < A_{crit} < 4$$

For the stability of the system a short delay time  $T_u$  is of primary importance. Because a reheater of the usual design heated with live steam results in a relatively long delay time and, moreover, long pipe lines have a particularly unfavourable influence upon stability owing to the pure dead time they cause, a cooling cycle without reheater and of a compact design, was selected as the starting point of this study.

These and similar measures result in a reduction in the energy storage capacity  $C$ . The lower limit is determined by the steam and water quantities in the evaporators. The development of a suitable evaporator is going on [5]. A low energy storage capacity has the consequence, that the cycle feedback starts not only as early as possible but also sufficiently strongly, so that the power rise and thus the increase in can temperature are controlled sufficiently fast. However, the energy storage capacity must not fall below a lower limit for reasons of stability.

Finally, the absolute value of the pressure gain  $K_p$  is kept small for safety reasons in order to cause the reactor power to increase as little as possible during a pressure decrease. In addition,  $K_p$  should be negative in order to have the cycle feedback occur in the right sense.

This results in these three requirements with respect to inherent stability:

- 1) The dead time  $T_u$  should be as short as possible.
- 2) The pressure gain  $K_p$  should be small in absolute terms, but negative.
- 3) The energy storage capacity  $C$  should assume an optimum value dependent on  $T_u$  and  $K_p$ .

In addition to the requirement of inherent stability there is that of inherent safety from accidents. Special accident risks of the steam-cooled breeder reactor are provided by the possible reverse flow of superheated steam into the core, the density reduction due to a leak in the cycle, and the unflooding accident. These accident risks are influenced by the design and arrangement of the cycle components and the water and steam volumes.

The influence of these parameters on stability and safety is investigated in this paper:

- Water and steam volumes in the evaporators
- Volumes of steam inlet- and outlet-plenum at the core
- Volume of water reservoir at core inlet
- Power density of fuel rods
- Number and characteristics of blowers
- Arrangement and design of blower turbines
- Arrangement of cooling cycle inside or outside the reactor pressure vessel.

The effect of these parameters is investigated on the following disturbances:

- Reactivity disturbance
- Blower failure
- Load changes
- Rupture of superheated-steam pipe
- Rupture of saturated-steam pipe
- Unflooding accident.

### 3. DISTURBANCES

#### 3.1 Reactivity Disturbance

The effects of a reactivity disturbance were described qualitatively in [6]. Below it is shown on what quantities the disturbance behaviour depends and what the influence of an increase in rod power is quantitatively.

The reactivity gain  $K_k$  can be calculated from the relations for the reactivity feedback, because in the transient state the sum of disturbance reactivity  $\Delta k_d$  and reactivity feedback  $\Delta k_f$  must become zero:

$$\Delta k_d + \Delta k_f = 0 \quad (3)$$

For an approximative treatment it is sufficient to consider only the Doppler coefficient  $\alpha_D$  and the steam density coefficient  $\alpha_\rho$ . Then it holds that

$$\Delta k_f = \alpha_D \times (\vartheta_F - \vartheta_{F0}) + \alpha_\rho \times (\rho - \rho_0) \quad (4)$$

Here and below the symbols have these meanings:

$\vartheta_F$	fuel temperature
$\vartheta_{F0}$	fuel temperature before disturbance
$\vartheta_{st}$	steam temperature
$\rho$	steam density
$\rho_0$	steam density before disturbance
$c_p$	specific heat of the steam
$\dot{m}$	steam throughput per fuel rod
$q$	power per fuel rod
$R$	heat transfer resistance fuel/steam

All values are averaged over the core. From the heat transfer equations and the energy balance sheets we derive

$$\vartheta_F - \vartheta_{Fo} = \left( \frac{1}{2 \times c_p \times \dot{m}} + R \right) \times \Delta q \quad (5)$$

$$(\varrho - \varrho_o) = \frac{1}{2 \times c_p \times \dot{m}} \times \left( \frac{d\varrho}{d\vartheta_{st}} \right) \times \Delta q \quad (6)$$

From the equations (1) and (3 to 6) results finally the reactivity gain

$$K_k = \frac{\Delta q/q}{\Delta k_d} = - \left[ \frac{1}{q \times \alpha_D \times R + \frac{q \times \alpha_D}{\dot{m} \times 2 \times c_p} + q \times \alpha_\varrho \times \frac{1}{2 \times c_p \times \dot{m}} \times \left( \frac{d\varrho}{d\vartheta_{st}} \right)} \right] \quad (7)$$

On the basis of this equation the main influencing quantities will be discussed now.

The first two terms and the last one in the denominator have a reversed sign.  $K_k$  is positive and the core is stable, if the first two terms which characterize the Doppler feedback are absolutely larger than the last term which gives the feedback of steam density. By reducing  $K_k$ , i.e. increasing the first two terms or reducing the last term, it is possible to improve the stability. A possibility which is accompanied with economic advantages is the increase in rod power with a simultaneous increase in the steam throughput per channel so that inlet and outlet temperatures remain unchanged [4].

Because of the simultaneous increase in  $q$  and  $\dot{m}$  the last two terms in the denominator of Eq. (7) remain unchanged, while the first term becomes larger.

Fig. 3 shows how the reactivity gain  $K_k$  becomes smaller with increasing rod power. Besides  $K_k$  the Doppler coefficient  $\alpha_D$  has been plotted which becomes smaller because of the higher average fuel temperature with increasing rod power. Yet, the Doppler feedback is increased because in the case of disturbance the absolute changes in fuel temperature are higher.

The high rod power required in the interest of low fuel cycle costs therefore at the same time contributes to the stability of the reactor. However, the increase of rod power must not result in exceeding the permissible temperature and stress of the casing. So, a precondition of an increase in power density is the intensification of heat transfer and the reduction of the hot channel factor, which can be achieved by cross mixing. These requirements are met by the fuel element schematically shown in Fig. 4, which was developed specially for the steam-cooled fast breeder reactor. It is characterized by casing tubes with six integral helical fins which serve simultaneously the purpose of spacing and cross mixing. Experiments proved that in this way and by application of surface roughening even in the case of steam cooling, rod powers of 600 W/cm at maximum can temperatures between 600 and 650°C can be achieved.

### 3.2 Blower failure

Being movable parts, the blowers must be regarded as being potentially susceptible to failure. Hence, special attention should be paid to the effects of the failure of a blower.

After the failure of a blower the pressure in the inlet plenum of the reactor decreases, because less steam is supplied. In the outlet plenum the pressure rises because of the reduced steam removal.

The reduced pressure head then results in a reduced steam throughput through the core. The consequence is an increased heating of the steam so that the average density of the steam decreases, while the reactivity increases. This causes the power of the reactor to rise. This power rise is limited to a value which is the lower,

- 1) the smaller the power gain of the core due to a density reduction,
- 2) the more blowers are used that is, the less the missing quantity of supply matters in terms of percentage,
- 3) the flatter the blower characteristics, since with decreasing supply pressure the blowers still operating will supply more than in the case of steep characteristics,
- 4) the larger a water reservoir kept at boiling temperature and connected with the inlet plenum, because it will slow down by evaporation the pressure decrease,
- 5) the faster the system pressure rises after the power increase of the reactor, i.e. the shorter delay time and capacity of the cycle are.

Fig. 5 shows the time behaviour of the steam quantity delivered, of reactor power and of the can temperature after failure of one blower. Number and characteristics of the blowers are varied.

The upper diagram shows the reduction in the steam flow through the core, which is much more pronounced with four blowers than it is with six. Moreover, it shows how much the delivery of the still operating blowers increases. Because of its flatter characteristics the radial blower proves to be superior to the axial blower.

As the diagram in the middle shows, the reactor power increases the more the larger the reduction in the steam mass flow.

As is shown by the lower diagram, the can temperature rises in the case of four axial blowers within some 5 seconds from  $585^{\circ}\text{C}$  by  $160^{\circ}\text{C}$  to  $745^{\circ}\text{C}$ , not taking into account the hot channel factor. When the number of blowers is increased from four to six, it only rises by  $105^{\circ}\text{C}$  to  $690^{\circ}\text{C}$ . When six radial blowers are used instead of six axial ones, the maximum of the can temperature is additionally reduced by  $25^{\circ}\text{C}$ .

A further decrease in the rise of reactor power and can temperature can be achieved by a reduction in the energy storage capacity  $C$  of the cycle. Fig. 6 shows that a reduction of this capacity from 750 to  $325 \frac{\text{MWs}}{\text{atm}}$  results in an overshooting of the pressure at the reactor outlet by 1 atm, but that it also reduces the maximum of the canning temperature by another  $25^{\circ}\text{C}$ .

In the case of a failure of one of four radial blowers a realistic energy storage capacity of the cycle will result in a short-time rise of the can temperature by about  $100^{\circ}\text{C}$ . The increase in stress caused by this temperature rise is most dangerous on the inside wall of the fuel element can. Under the adverse assumption that the steam temperature does not change, the short-time stresses produced on the inner wall of the can were determined. In case of a temperature step of  $100^{\circ}\text{C}$ , at the beginning as well as at the end of the life of the can, they remain some  $15 \frac{\text{kp}}{\text{mm}^2}$  below the yield strength if Inconel 625 is used, taking into account the hot channel factor. Hence, the temperature step produced by the restriction to four blowers does not entail an undue load on the canning.

Nevertheless, the aim of development was to achieve high operational safety of these blowers. Fig. 7 shows how this was safeguarded by an overhung arrangement of a centripetal turbine and a centrifugal blower on a shaft equipped with condensate-lubricated bearings. Such an enclosed design reduced the problem of leakage to insignificant proportions and avoided contamination of the cycle by a lubricating agent other than the working medium. Two prototype blowers of this type have proved their reliability on the test bed [9].



### 3.3 Load Changes

If the power consumption and the steam requirement of the main turbine change, the reactor power is to follow this change as rapidly as possible. If the aim is an inherently good load following behaviour, this requirement must be harmonized with inherent safety from a superheated-steam pipe rupture, as will be explained later.

Fig. 8 shows the time behaviour of the reactor power after a 10% increase in the steam consumption of the main turbine. First, the reactor power will decrease because, owing to the higher throughput through the core, the steam will not be heated to such an extent and its density will increase. Later on, the reactor power will increase again, since with a decrease in system pressure also the steam density will decrease. The power increases until finally 110 % of the initial value have been reached, i.e. exactly the value which is taken from the main turbine.

The initial reduction in power is more pronounced if series turbines are used as blower drive (curves B,C,D) than in the case of parallel turbines (curve A). This is due to the fact that the whole steam quantity flowing to the main turbine, which is increased when the load is higher, flows through the series turbines. The power of the turbines and thus the quantity supplied by the blowers into the core increase. This results in an additional increase in steam density and hence in a reduction of reactivity and reactor power. In an otherwise identical cooling cycle it will take more time therefore for series turbines to reach the desired power increment than for parallel turbines, as is shown by Curves A and B. The load following behaviour, however, can be much improved by reducing the water reservoir (Curve C) and the capacity of the cycle (Curve D).

### 3.4 Rupture of a Superheated-Steam Pipe

The behaviour of the reactor in case of a rupture of a superheated-steam pipe qualitatively equals the behaviour in load increase of the main turbine, because in both cases a major steam quantity is taken from the outlet plenum and because it is the same to the reactor whether this flows to the main turbine or through a leak. A qualitatively different behaviour would be desirable, since in increasing the turbine load the power of the reactor should follow the increased demand as rapidly as possible, whereas the power should drop as soon as there is a rupture of a superheated-steam pipe. These conflicting requirements to inherent safety from the consequences of the rupture of a superheated-steam pipe, on the one hand, and inherently good load following behaviour, on the other hand, result in contrary design tendencies which will be explained below.

Fig. 9 shows the time plot of the reactor power following a rupture of a superheated-steam pipe. As in an increase in the steam quantity on the main turbine, the reactor power first drops. The blower drives considered here are parallel turbines. When using series turbines the initial power drop would be more pronounced (cf. Fig.8). Afterwards, the power will increase the more rapidly the bigger the quantity leaking out (Curves A,B,C) and the lower the energy storage capacity of the cycle (Curve D). This shows the significance of an effective limitation of the leakage quantity.

In a desintegrated design or if the blowers are driven by parallel turbines, the quantity leaking out must be limited by Venturi nozzles. Such Venturi nozzles are used for the KRB boiling water reactor at Gundremmingen. In the case of a steam cooled fast reactor a more economic and effective limitation of

the leakage quantity can be realized by an integrated design coupled with the use of series turbines as the blower drive. As long as the pressure vessel is intact, leaks are then possible only behind the series turbine, the nozzle ring of which is designed always to operate with high steam velocities.

Since this velocity cannot rise to more than the velocity of sound, this is an automatic and effective limitation of the steam flow. Moreover, as contrary to the use of Venturi nozzles, no additional pressure loss has to be taken into account, the steam flow can be limited to 1.3 times the design value by a suitable design of the series turbines, which reduces the effects of the rupture of a superheated-steam pipe to insignificant proportions.

Another advantage of the series turbine is its ability to supply a fast shutdown signal for the reactor by the strong increase in blower speed already at a time at which the reactor power has not yet risen above the design value.

### 3.5 Rupture of a Saturated-Steam Pipe

In this section the following pipe ruptures are investigated with respect to their effect:

- 1) Saturated-steam pipe between blower and inlet plenum
- 2) Simultaneous rupture of saturated and superheated-steam pipe in the case of concentric pipe design.

In a reactor with ~~des~~integrated layout in which all cycle components are arranged independent of each other outside the reactor pressure vessel and interconnected by pipes all

steam pipes are loaded by the full pressure. In this case the average steam density in the core will decrease faster following a rupture in the saturated-steam line than due to the rupture of a superheated-steam line, because in the first case the pressure as well as the coolant flow through the core decrease, while in the second case the pressure decreases, but the coolant flow increases and consequently the average steam temperature decreases.

In the rupture of only the saturated-steam pipe the pressure on the inlet side may become smaller than that on the outlet side, so that the direction of flow reverses. The inflow of superheated steam will cause the rate of density change to rise very steeply. This reversal of flow occurs the earlier the larger the evaporator volumes, because in case of a pressure decrease the evaporation in the evaporators delays the pressure decrease on the outlet side of the reactor. Since the water volume  $V_{ew}$  and the steam volume  $V_{es}$  reduce the reduction of pressure in the evaporators in qualitatively the same way, these two volumes were combined in the volume  $V_e$ .

$$V_e = V_{ew} + V_{es}/R$$

The constant  $R$  is determined so that  $R \text{ m}^3$  steam in a pressure decrease have the same volume increment as  $1 \text{ m}^3$  of water.

Fig. 10 shows the influence on the rate of density reduction of the steam and water storage volumes at the core inlet  $V_i$  and outlet  $V_h$ . Water and steam volumes at core inlet were combined to  $V_i$  in a corresponding way as in the case of  $V_e$ . With large  $V_i$  the size of  $V_h$  has only a slight influence upon  $\frac{d\rho}{dt}$ . This influence increases strongly with decreasing  $V_i$ . The larger  $V_h$ , the more

slowly the pressure will decrease at the core outlet and the faster the pressure difference between core inlet and outlet will be reduced. This results in a reduction in steam flow through the core and thus in a higher steam temperature.

If  $V_h$  exceeds or  $V_i$  falls below a certain value, the pressure at the outlet exceeds that at the inlet and the direction of flow will be reversed. If a certain maximum rate of density change is postulated, Fig. 10 will indicate pairs of values of  $V_i$  and  $V_h$  which permit these limits to be kept by design measures. This limit can be shifted in the direction of smaller volumes by reducing the evaporator volumes  $V_e$ . Such limit for  $V_e = 70 \text{ m}^3$  is shown in Fig. 11 for a  $\frac{d\rho}{dt} = 90 \text{ kg/m}^3\text{sec}$ , which corresponds to a ramp slope of 10  $\$/\text{sec}$ .

Even if there is no flow reversal at full power, this may well be the case under partial load. Fig. 12 shows the dependence of the rate of density reduction on the steam mass flow at 50 % partial load for three different evaporator volumes. In both cases the rate of density reduction increases with decreasing mass flow. Such decrease of mass flow is required to maintain a constant steam temperature at partial load. In the case of the evaporator volume of  $V_e = 200 \text{ m}^3$  the curve of the rate of density reduction in principle shows a different behaviour than that at  $V_e = 50 \text{ m}^3$ , which is due to the flow reversal brought about with the large evaporator volume. If a maximum ramp slope of 10  $\$/\text{sec}$  is permitted, which roughly corresponds to a rate of density reduction of  $\frac{d\rho}{dt} = 90 \text{ kg/m}^3 \text{ sec}$ , the volume of the evaporators must be kept very small in the desintegrated design and in the case of the realistic values for the inlet- and outlet-volumes adopted as the basis of the diagram it must not exceed  $70 \text{ m}^3$ .

In a partially integrated design in which the components of every partial cooling cycle are combined in one unit each and connected with the reactor by concentrically arranged superheated and saturated-steam pipes, only the outer saturated-steam pipes have to withstand the load by the operating pressure. The superheated-steam pipes on the inner side are designed only for the differential pressure and will consequently also rupture in case the outer saturated-steam pipes should rupture. The outlet volume  $V_h$  and the evaporator volume  $V_e$  in that case have a very small influence on the rate of density change. If these volumes are very small, the pressure at the core outlet will decrease more quickly, but this results in a larger steam flow through the core and thus in a smaller average steam temperature. As the calculations have shown the influences of pressure and temperature about balance each other. However, the inlet volume  $V_i$  is of decisive importance, as is shown in Fig. 13. If the rate of density reduction brought about is not to exceed  $90 \text{ kg/m}^3 \text{ sec}$ , the inlet volume must be  $V_i > 40 \text{ m}^3$ .

Fig. 14 is a plot of the rate of density change as a function of the number of blowers. It is seen that this influence is very much stronger in the case of a partially integrated and especially of desintegrated designs and, moreover, that the resulting rate of density change is larger by several orders of magnitude than in a fully integrated design coupled with the use of series turbines as the blower drive.

The fact that the integrated design can avoid the rupture of a saturated-steam pipe and the rupture of a superheated-steam pipe results in a very low rate of density reduction demonstrates the importance of the integrated design, especially in the case of steam-cooled fast breeder reactors.

The requirement of integration and adequate accessibility to the individual components result in a pressure vessel of prestressed concrete, owing to the high pressure of about 150 at and the status of the present technology. The layout of such a plant is shown in Fig. 15 and 16. The centrally arranged core is freely accessible from the top and the bottom, so that the refuelling can be carried out without any injury by the control rod system below the core. The conventional control system, shown in the figure, can be replaced by a fully-hydraulic operated system which requires only a few pipe penetrations of small diameter through the pressure vessel. Such a hydraulic control system is being developed and described in [10]. The evaporators and the steam blowers are arranged around the core and connected with it by short pipes. An integral layout like this therefore permits small volumes and thus the desired short delay and dead times.

Fig. 17 shows a comparison of the volumes required to ensure inherent stability with those obtained by the arrangement selected. This shows that the realized volumes satisfy the requirements of inherent stability. If these are met and an integrated design is adopted, the preconditions for inherent accident safety are provided as well.

### 3.6 Unflooding Accident

The integrated layout of the cooling cycle shown in addition permits good accessibility to the individual components, especially to the core. Loading and unloading of the core is performed at full sight in the flooded state. The transition from this state to power operation may be the cause of another accident because the reactor may become prompt-critical by unflooding under certain circumstances. As is shown in [1], this unflooding accident, which will be treated below, can result in unlimited reactivity ramps. By 'unlimited' we mean that these reactivity ramps, unless controlled by the scram system, will lead to a Bethe Tait excursion which is finished by the disassembly of the core. It will be shown below how it is possible to limit the maximum possible reactivity ramps of these accidents inherently by suitable arrangement and dimensioning of the cooling cycle.

Fig. 18 shows the dependence of reactivity on the coolant density. Curve A was taken from the D-1 Study [2] and holds for a coolant homogeneously distributed throughout the core. One of the preconditions of the unflooding accident is that the reactivity of the flooded core, which is below -15 to -20 % normally (Curve A, Fig. 18), has been increased by mistake to such a level as to make the core go critical during unflooding (Curve B). Such increase in the reactivity of the flooded core is possible by overloading the core during refuelling or by erroneous withdrawal of control rods.

If the cooling cycle, which is pressurized and at boiling temperature, is opened, e.g. by maloperation of a valve, a water-steam mixture of a critical mass flow will flow out. This critical mass flow of a two phase flow corresponds to the flowing out of a single phase flow at sonic velocity. This maximum possible



mass flow was calculated by the theory of Moody [11]. If the outlet opening is below the water level, there will be very rapid unflooding of the core. In the case of the reactivity curve B, Fig. 18, this results in very steep reactivity ramps. To preclude these from arising, it must be safeguarded by the design that no steam lines penetrate the pressure vessel below the water level in the flooded condition.

Unless this requirement is met, the conditions shown in the model on Fig. 19 may come about. The leakage causes the pressure in the system to drop. This produces steam bubbles in the water so that the average specific volume increases. This has a positive effect on the outlet plenum  $V_h$ , because in this way the reduction of the water level is slowed down. However, it has an adverse effect on the water reservoir  $V_w$ , because its evaporation slows down the further pressure reduction and thus the continued evaporation in  $V_h$ . Thus it appears that  $V_h$  and  $V_w$  will have contrary effects in an unflooding accident.  $V_h$  should be large while  $V_w$  should be small in order to prolong the unflooding time.

In the calculatory treatment it is assumed by way of approximation that in unflooding the average coolant density in the core changes with a constant average speed. This shall be defined as follows:

$$\left(\frac{d\rho}{dt}\right)_m = \frac{\rho_w - \rho_{st}}{\Delta t} \quad \left[ \frac{\text{kg}}{\text{m}^3 \text{ s}} \right]$$

$\rho_w \left[ \frac{\text{m}^3}{\text{kg}} \right]$       Density of the water with the reactor flooded

$\rho_{st} \left[ \frac{\text{m}^3}{\text{kg}} \right]$       Density of the steam with the reactor unflooded

$\Delta t \left[ \text{s} \right]$       Flow time for unflooding the core

If the rate of density change is calculated by the above equation, it turns out that the effect of the smaller mass flow at lower pressure is compensated in part by the greater difference in density between water and steam. This explains the flat peak of the curves in Fig. 19 in which  $(\frac{d\rho}{dt})_m$  was plotted as a function of pressure and of the storage volume at the core inlet  $V_i$ . Here,  $V_i$  is a combination of  $V_s$  and  $V_w$  in correspondence with Section 3.5.

To obtain the reactivity ramp from the rate of density change,  $(\frac{d\rho}{dt})_m$  must be multiplied with the coolant density coefficient  $(\frac{dk}{d\rho})_m$ . This is shown by Fig. 18 to depend on the steam density. From this figure it is evident that the slope of the reactivity curve increases with decreasing density. The reactivity ramp  $\frac{dk}{dt}$  therefore will be particularly large in an unflooding accident if the reactor becomes critical only at small density.

However, it should be considered in the determination of the coolant density coefficient that about 5 to 10 % reactivity, depending upon the initial temperature, must be introduced into the core to heat the fuel up to evaporation. The average coolant density coefficient during the introduction of this reactivity therefore is the highest if the reactivity curve is displaced upward just so much as to make the unflooded reactor some 5 % supercritical (reactivity curve B in Fig.18).

For these reasons, a  $(\frac{dk}{d\rho})_m$  was determined for the different pressures which is defined as follows:

$$\left(\frac{dk}{d\rho}\right)_m = \frac{\Delta k}{\Delta \rho} = \frac{5 \text{ \%}}{\rho_{st} - \rho_{crit}}$$

Here,  $\rho_{crit}$  was chosen so that the reactivity at this density is smaller by 5 % than at  $\rho_{st}$ . Fig. 20 shows the calculated reactivity ramp as a function of pressure. It reaches a maximum around 50 atm which is less than twice as high as the value at 150 atm. Therefore, a pressure of 50 atm will be used as the most unfavourable case in the calculations below.

Fig. 21 shows the rate of density change ( $d\rho/dt_m$ ) as a function of volumes  $V_h$  and  $V_i$  under the assumption of a leak of  $400\text{ cm}^2$ . The restriction of the leakage cross section to such a small value is only possible by using series turbines as blower drive. With rising  $V_i$  also  $d\rho/dt$  rises so that  $V_i$  may not be any arbitrary size because of the unflooding accident. For the size of  $V_h$  there is a theoretical optimum size as a function of  $V_i$ , but this is so high at practicable values of  $V_i$  as to make the delay time too long.

If an upper limit is fixed for the reactivity ramp and thus for the rate of density reduction in an unflooding accident, it is possible to read pairs of values of  $V_h$  and  $V_i$  from Fig. 21 which permit this limitation by design measures. Fig. 11 shows two limits for unflooding ramps of 30 and 40 %/sec. A reactivity ramp of 30 %/sec should not be exceeded essentially in order to avoid a can burst. This limitation requires a very large superheated-steam plenum  $V_h$ . This results in a delay time of the heat transport from the core to the evaporators which is undesirably long with respect to stability. This conflict between the requirements of stability and safety does not occur, however, if all steam lines penetrate the pressure vessel above the water level in the flooded condition. If there is an additional sufficiently large steam volume between the water level and the discharge opening, the unflooding rate and thus the highest possible reactivity ramp are decisively reduced without impairing the stability.

#### 4. CONCLUSION

It has been shown that with a negative steam density coefficient the feedback of the cooling cycle can be utilized to achieve inherent stability and safety from accidents. The limits to be observed in the design of the cycle were determined and were found to be implementable on the basis of a design example.

The corresponding development of the components disclosed no fundamental difficulties. Their joint operation in a closed cycle is the subject of a comprehensive experimental program. A loop specially built for this purpose is in operation.

In case these experiments were to confirm the analytical considerations described in this report, the requirements to engineered safeguards would be reduced and the selection of potential sites of steam-cooled breeder reactors would be made much easier.

## References:

- [1] ERBACHER F., FRISCH W., HÜBSCHMANN W., RITZ L., WOITE G.;  
'The safety of steam-cooled fast reactors as influenced  
by the design and arrangement of their components.'  
Proc. Internat. Conf. on Fast Reactor Safety,  
19-22, Sept. 1967, Aix-en-Provence; KFK 655, Oct. 1967
- [2] MÜLLER A.; 'Referenzstudie für den dampfgekühlten  
schnellen Reaktor (D-1)', KFK 392, August 1966,  
Kernforschungszentrum Karlsruhe
- [3] FRISCH W., WOITE G.; 'Analogrechenmodell für dampf-  
gekühlte schnelle Reaktoren mit Direktkreislauf'.  
(in Vorbereitung), KFK 657, Kernforschungszentrum  
Karlsruhe
- [4] KREBS L.; 'Die Stabilität von starr zurückgeführten  
Regelstrecken ohne Ausgleich am Beispiel eines dampf-  
gekühlten Reaktors'. KFK 656, Sept. 1967, EUR 3691d  
Kernforschungszentrum Karlsruhe
- [5] ERBACHER F., SCHMIDT H., WIEHR K.; 'Die Entwicklung  
von Verdampfern für dampfgekühlte Reaktoren'. EUR 3695d  
KFK 659, Oktober 1967 (in Vorbereitung),  
Kernforschungszentrum Karlsruhe
- [6] FRISCH W., HELLER F., HÜBSCHMANN W., MALANG S.,  
MÜLLER A., SCHIKARSKI W., SMIDT D., WOITE G.;  
'Safety Aspects of Steam-Cooled Fast Breeder Reactors'.  
KFK 613, June 1967, Kernforschungszentrum Karlsruhe

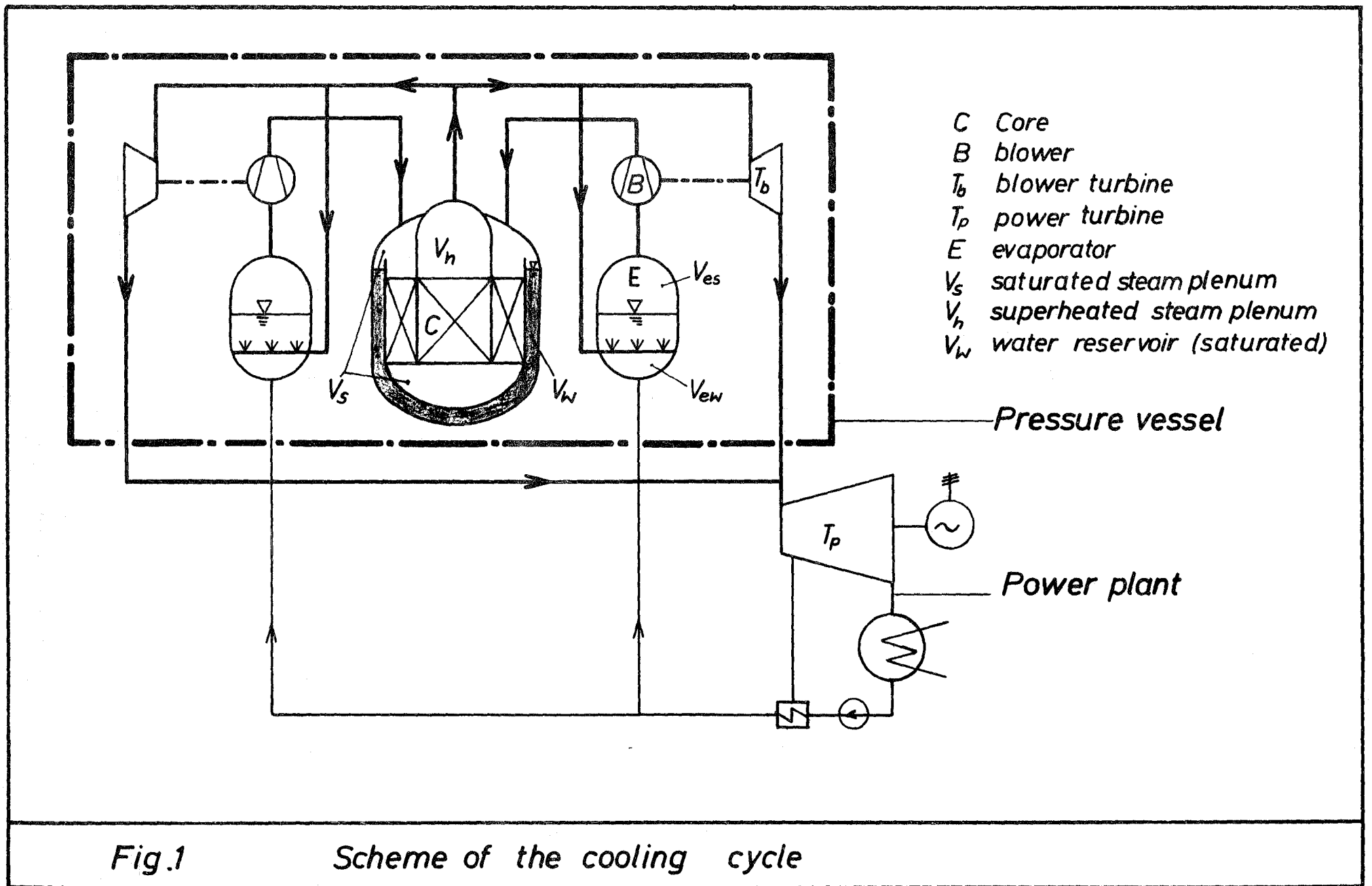
- [7] HOFMANN F., KIEFHABER E., MOERS H., SMIDT D.;  
'System Analysis of a fast steam-cooled reactor of  
1,000 MWe'. KFK 636, SM 101/10, October 1967,  
Kernforschungszentrum Karlsruhe
- [8] BAUMANN W., CASAL V., MÖLLER R., RITZ L., RUST K.;  
'Brennelement-Hüllrohre mit integralen Wendelrippen  
für dampfgekühlte Brutreaktoren'. KFK 658, EUR 3694d,  
November 1967, (in Vorbereitung). Kernforschungszentrum  
Karlsruhe
- [9] ERBACHER F., RADTKE F.; 'Die Entwicklung von Dampf-  
gebläsen für dampfgekühlte Reaktoren'. KFK 545,  
Februar 1967, Kernforschungszentrum Karlsruhe
- [10] MÜHLHÄUSER, O.: 'Zur Entwicklung eines vollhydraulisch  
betriebenen und gesteuerten Regel- und Abschaltsystems  
für wasser- bzw. dampfgekühlte Kernreaktoren'.  
KFK 665, EUR 3699, August 1967, Kernforschungszentrum  
Karlsruhe
- [11] MOODY F.J.; 'Maximum Flow Rate of a Single Component,  
Two Phase Mixture'. Journal of Heat Transfer,  
Trans. ASME, Series C. Vol. 87, 1965
- [12] HÜBSCHMANN W.; 'Grenzreaktivitätsrampen im dampfge-  
kühlten schnellen Reaktor'. KFK 664, EUR 3682d,  
November 1967, (in Vorbereitung), Kernforschungszentrum  
Karlsruhe.

Figures:

- 1 Scheme of the cooling cycle
- 2 Power transient following an 0.2  $\beta$  reactivity step
- 3 Relative changes of Doppler coefficient and reactivity gain versus rod power
- 4 Diagrammatic view of the fuel element
- 5 Influence of number and type of blowers on cycle dynamics after blower failure
- 6 Influence of the capacity of the cycle on cycle dynamics after blower failure
- 7 Turbine driven steam blower
- 8 Rate of power change following a 10 % load increase
- 9 Rate of power change due to rupture of superheated-steam pipe
- 10 Density reduction rate as caused by rupture of saturated-steam pipe and influenced by the volumes
- 11 Design range of volumes as limited by acceptable reactivity ramps
- 12 Density reduction rate as caused by rupture of saturated-steam pipe at 50 % load
- 13 Density reduction rate as caused by simultaneous rupture of the superheated and saturated-steam pipes and influenced by the inlet volume
- 14 Density reduction rate as caused by various pipe ruptures and influenced by the number of blowers

- 15 Arrangement of an integrated cooling cycle for a 1,000 MWe steam-cooled fast breeder reactor (longitudinal cross section)
- 16 Arrangement of an integrated cooling cycle for a 1,000 MWe steam-cooled fast breeder reactor (horizontal cross section)
- 17 Volumes as realized by an integrated cooling cycle for a 1,000 MWe steam-cooled fast breeder reactor
- 18 Reactivity versus steam density
- 19 Density reduction rate of unflooding accident as influenced by the pressure
- 20 Reactivity **rate** of unflooding accident as influenced by the pressure
- 21 Density reduction rate of unflooding accident as influenced by the volumes





	A	B	C
$K_k$	2,2	1,09	0,685

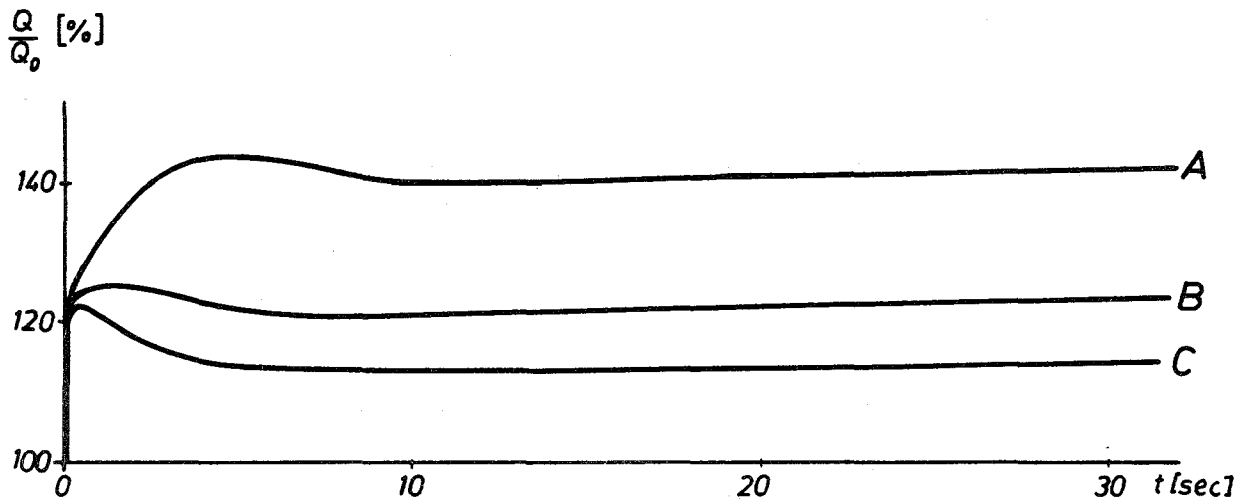


Fig. 2a Reactor power without feedback of the cooling cycle

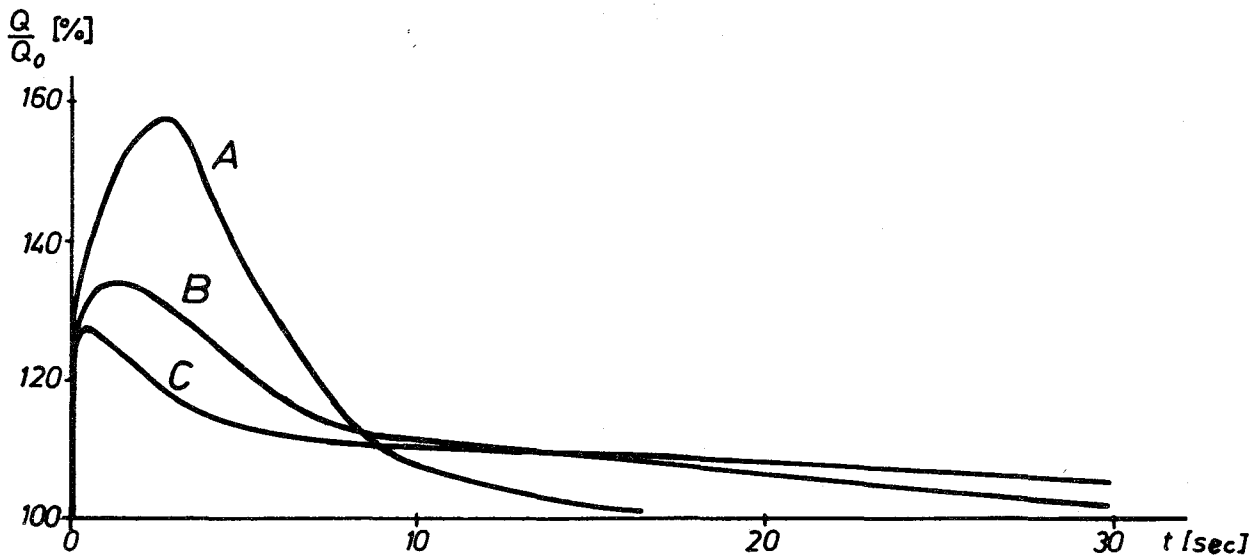
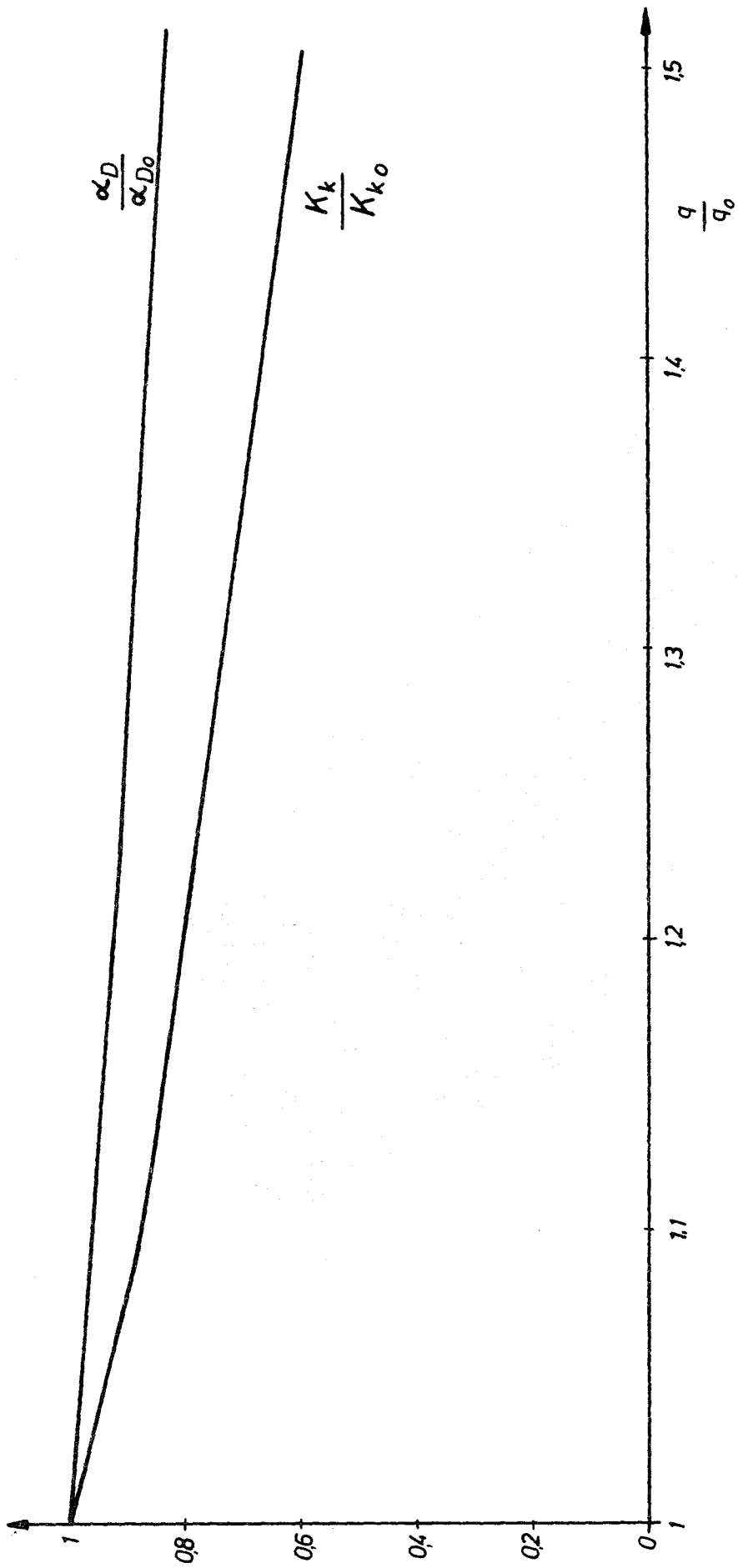
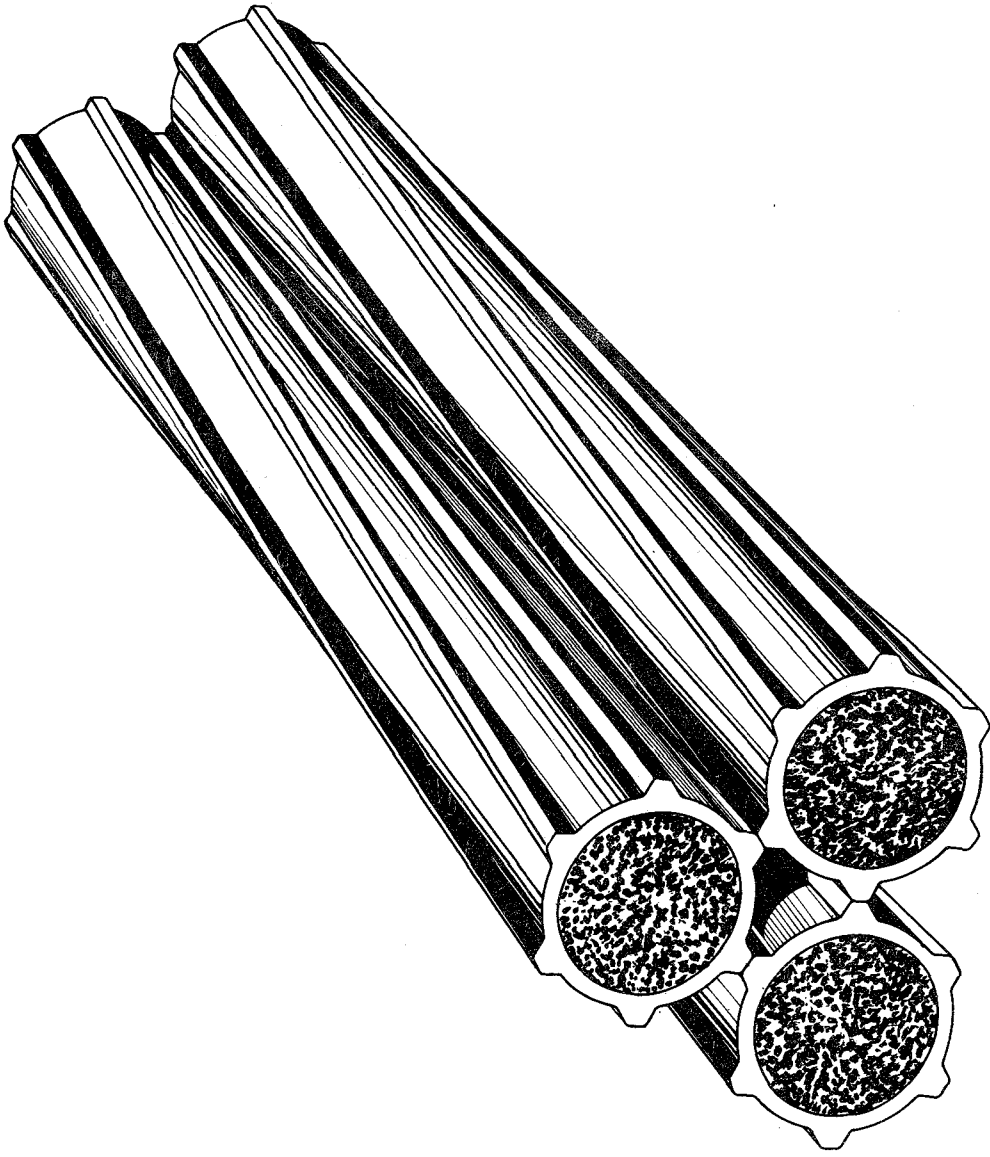


Fig. 2b Reactor power with feedback of the cooling cycle

Fig. 2 Power transient following an 0.2 \$ reactivity step



**Fig.3** Relative changes of Doppler coefficient and reactivity gain versus rod power



*Fig. 4 Diagrammatic view of the fuel element*

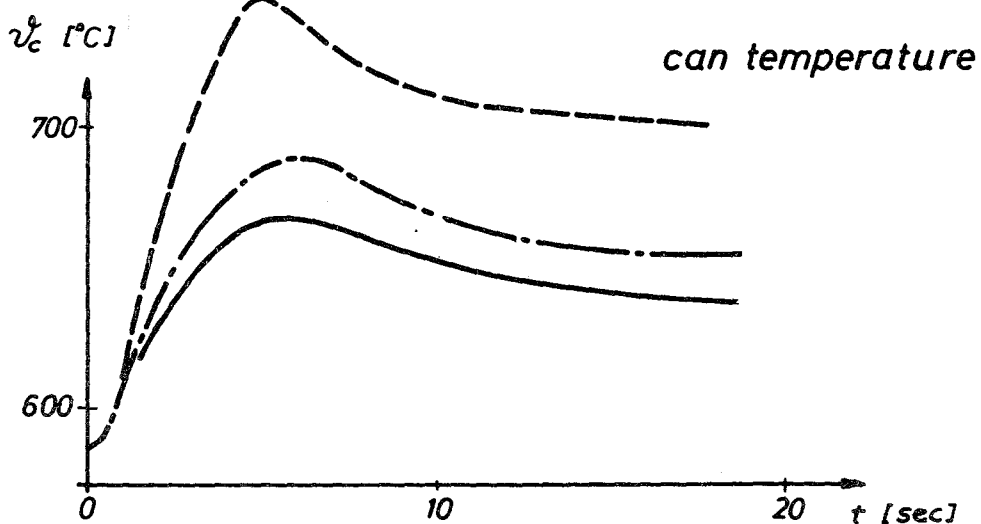
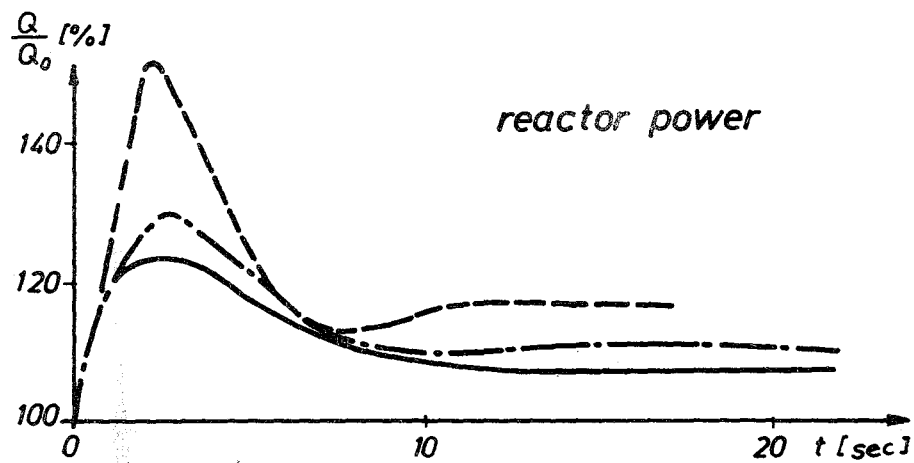
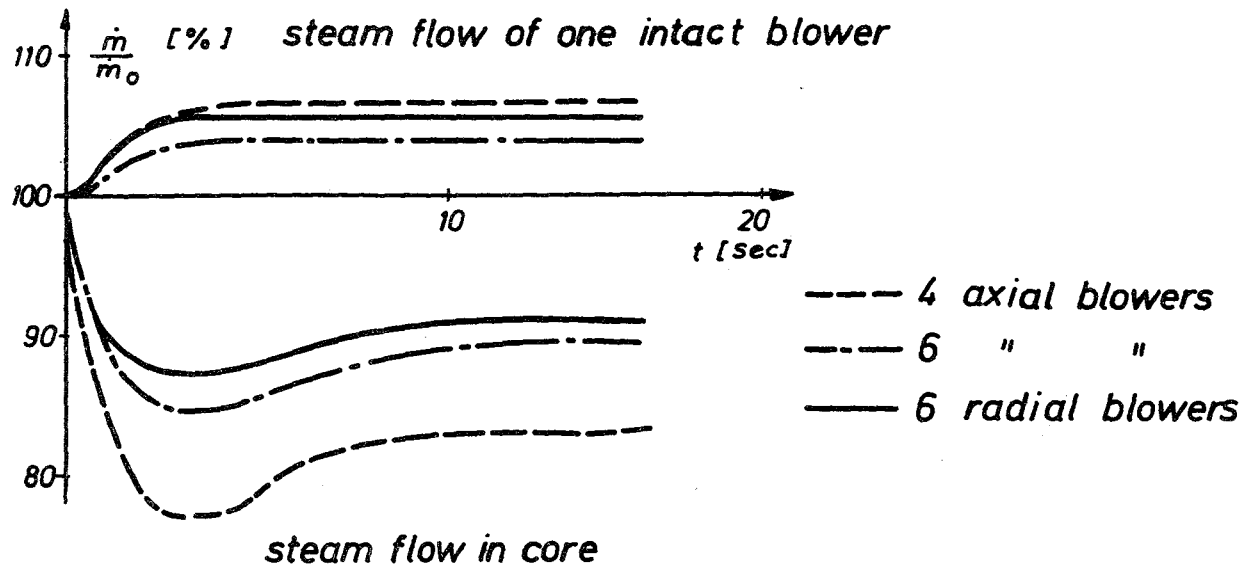
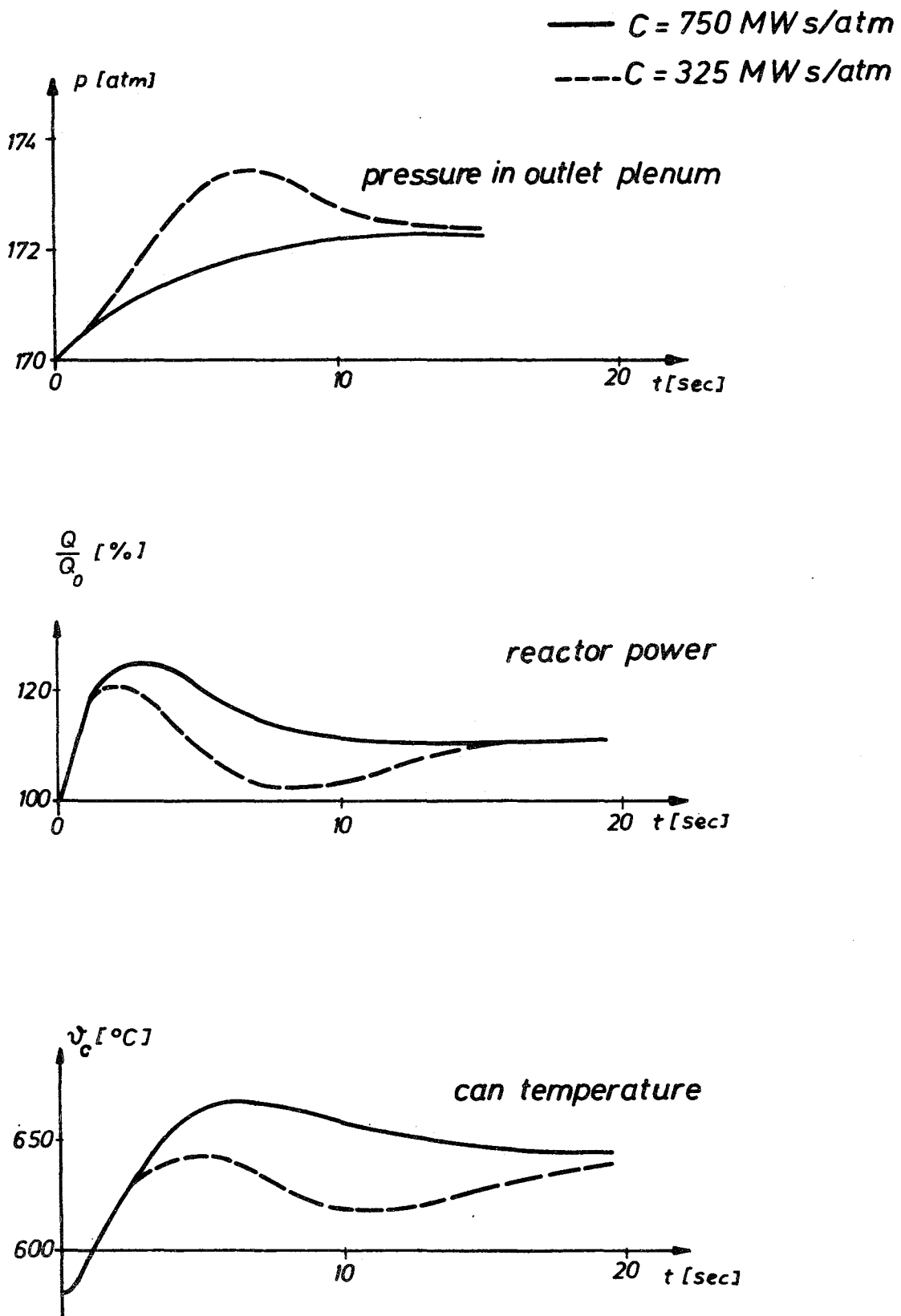


Fig. 5 Influence of number and type of blowers on cycle dynamics after blower failure



**Fig. 6** Influence of the capacity of the cycle on cycle dynamics after blower failure

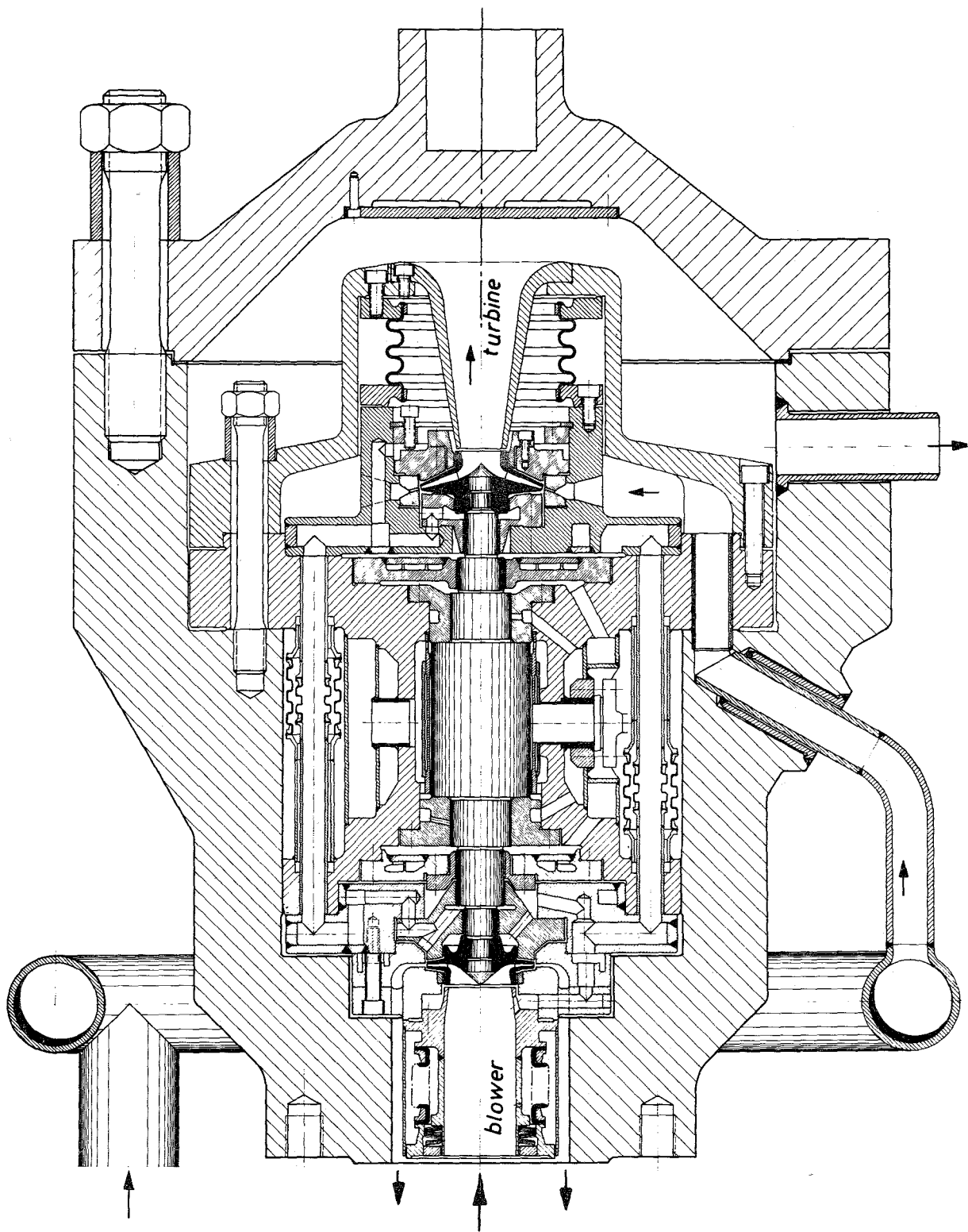


Fig. 7 Turbine driven steam blower

	A	B	C	D
energy storage capacity $C$ [MWs/atm]	750	750	750	325
water reservoir $V_w$ [ $m^3$ ]	400	400	0	50
arrangement of blower turbine	parallel	series	series	series

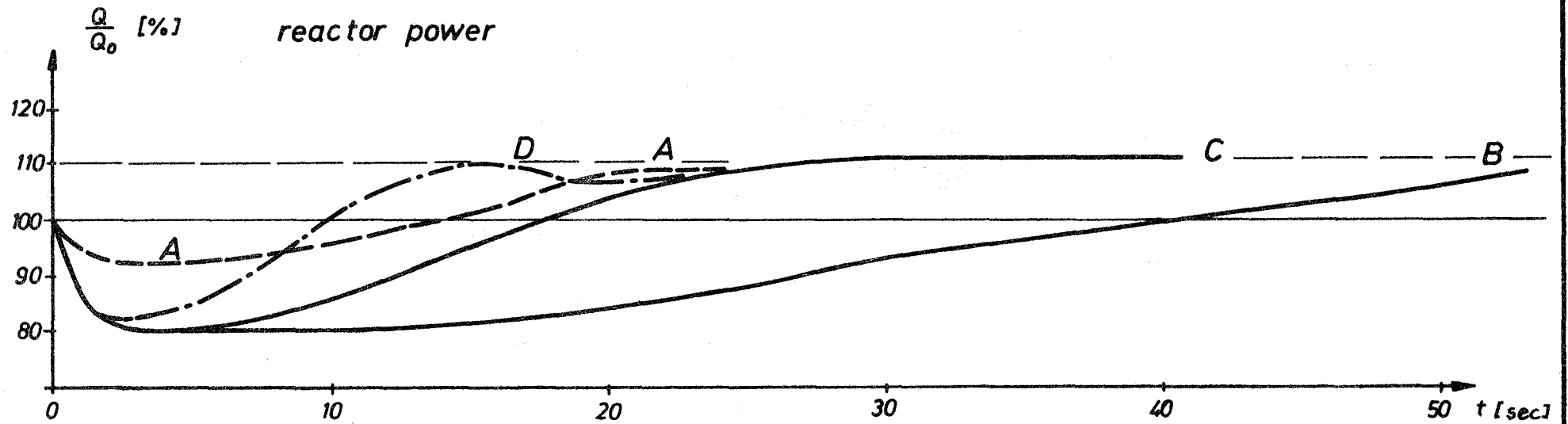


Fig.8

Rate of power change following a 10% load increase



	A	B	C	D
energy storage capacity $C$ [MWs/atm]	750	750	750	325
water reservoir $V_w$ [ $m^3$ ]	400	400	400	50
leaking steam flow [ $\frac{kg}{s}$ ]	112	225	450	450

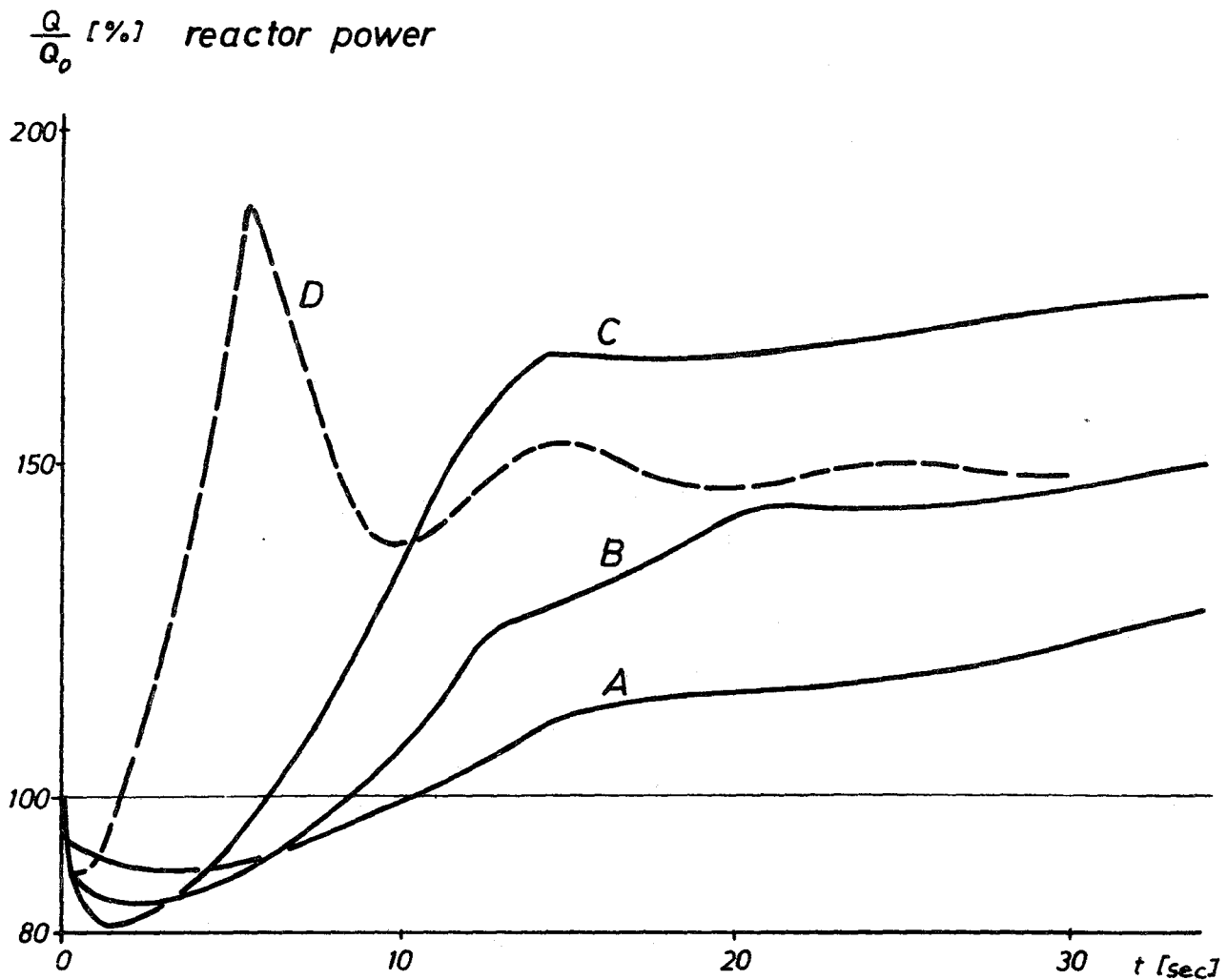


Fig. 9 Rate of power change due to rupture of superheated steam pipe

$$\left(\frac{d\rho}{dt}\right)_m$$
$$\left[\frac{\text{kg/m}^3}{\text{sec}}\right]$$

leak cross section  $F = 0,3 \text{ m}^2$   
evaporator volume  $V_e = 70 \text{ m}^3$

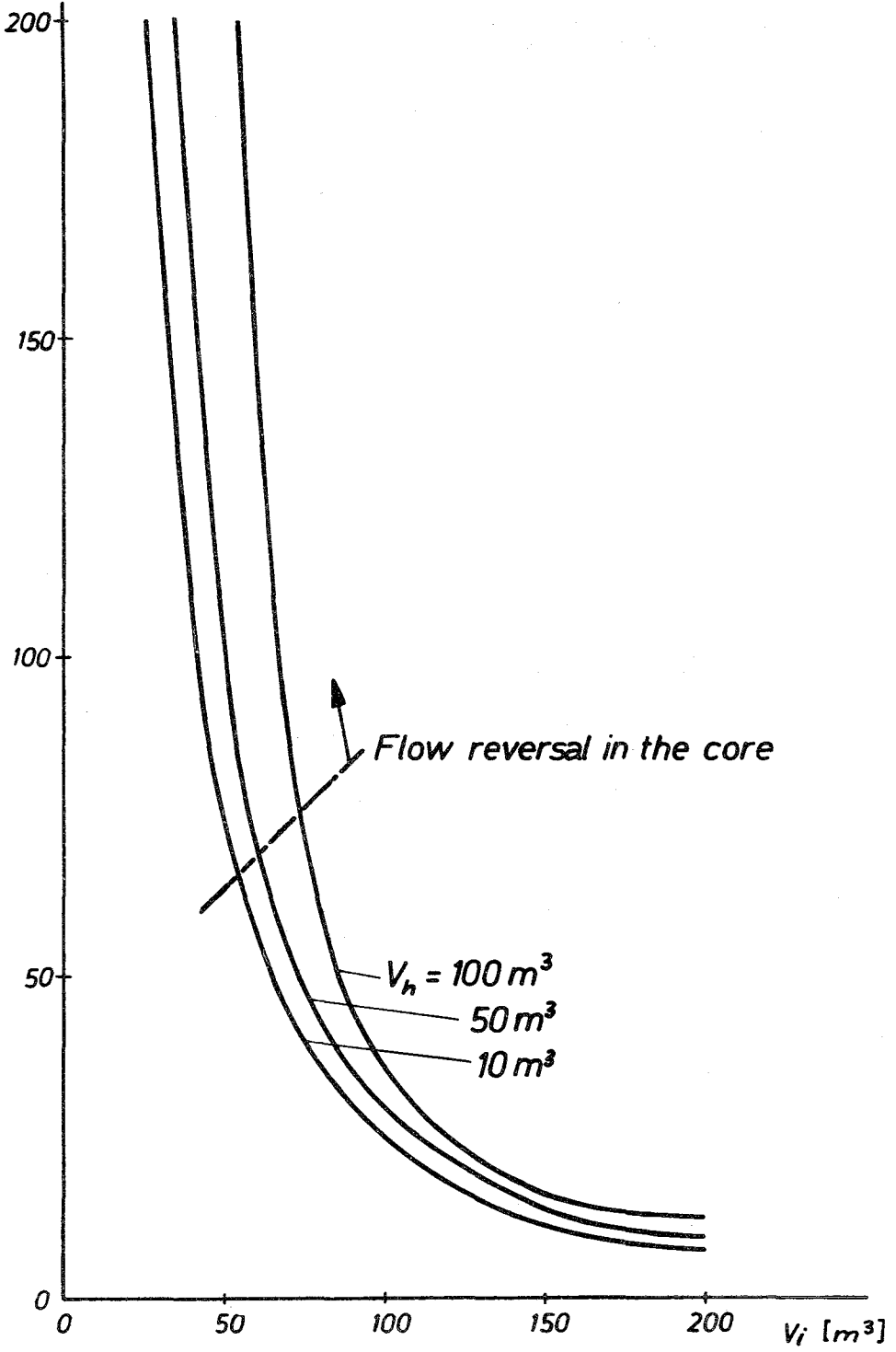
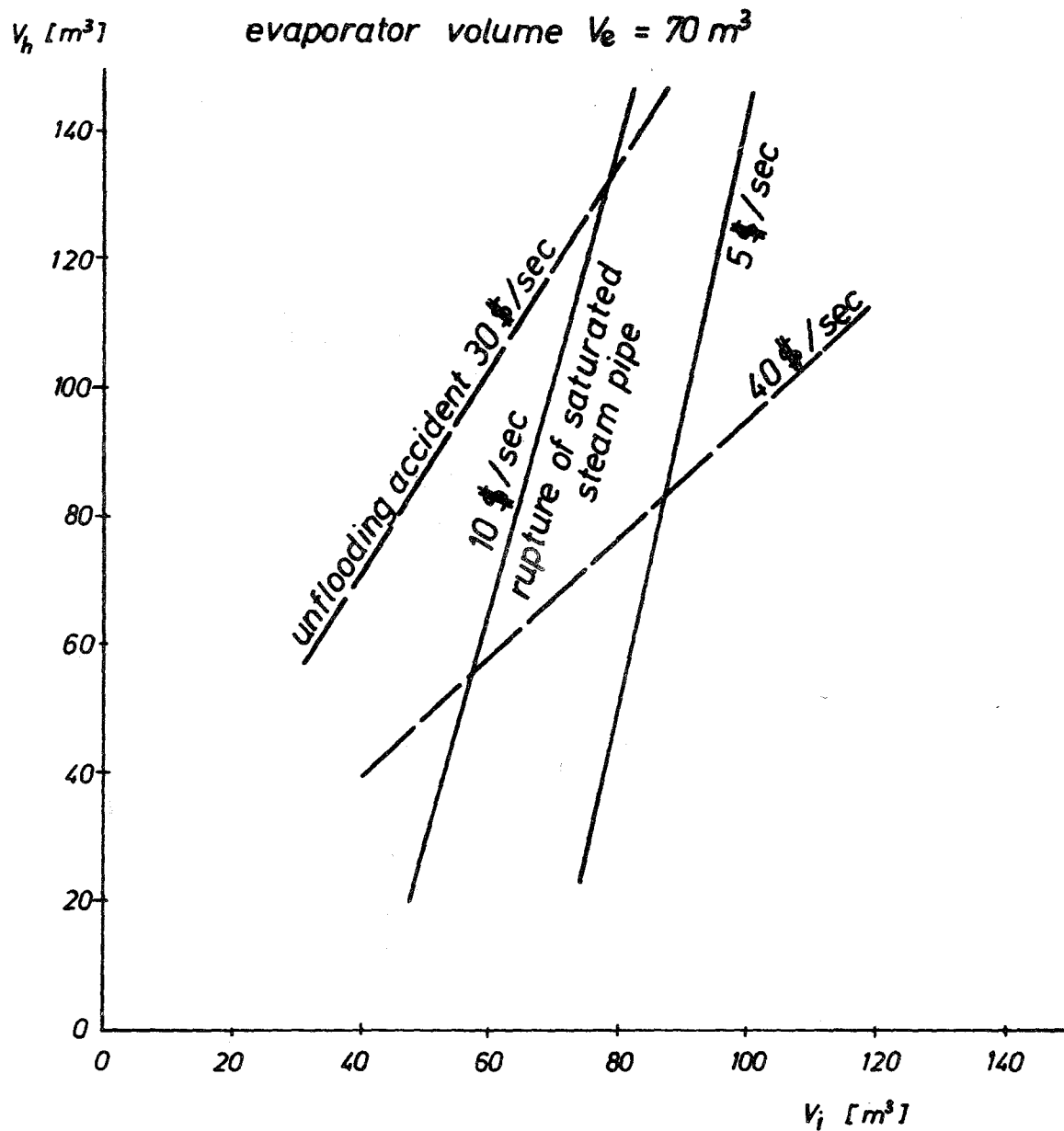


Fig.10 Density reduction rate as caused by rupture of saturated steam pipe and influenced by the volumes



**Fig.11** Design range of volumes as limited by acceptable reactivity ramps

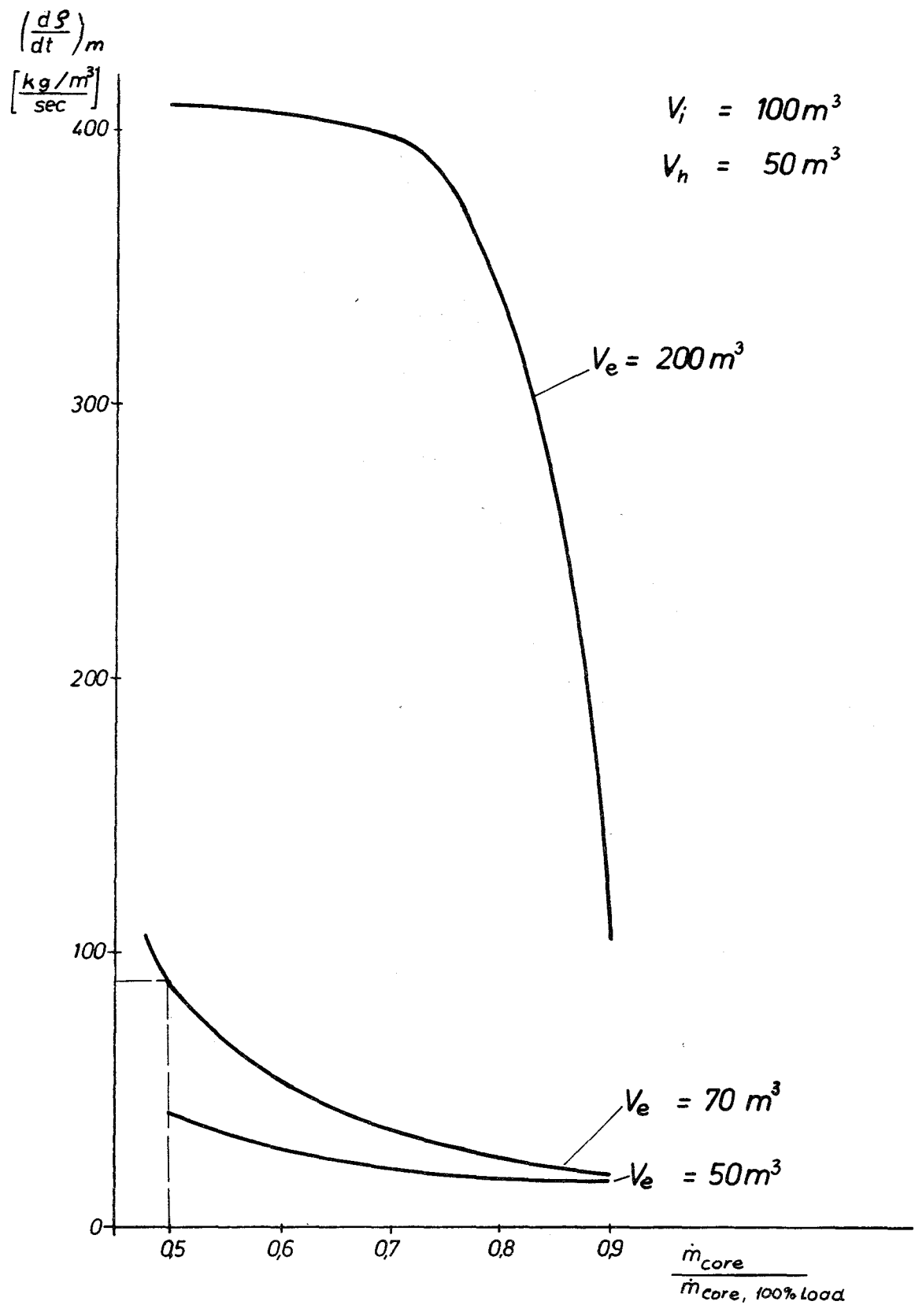
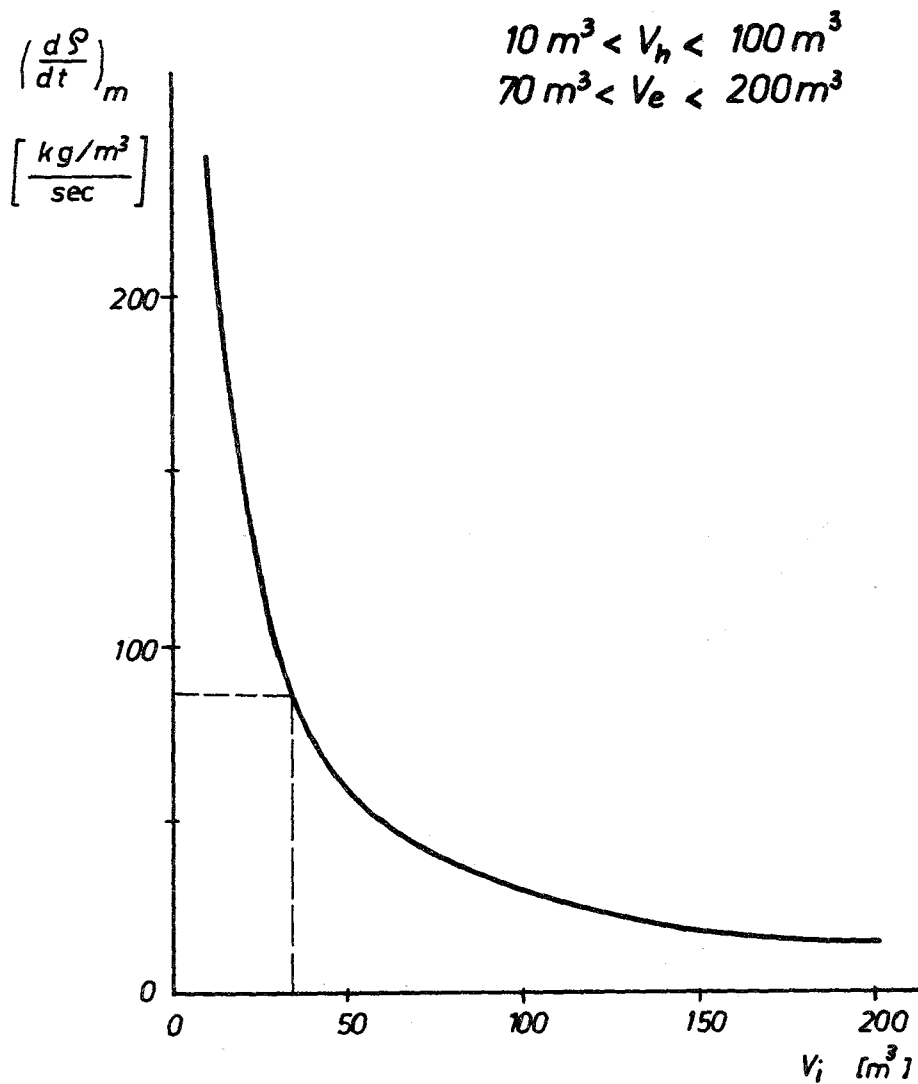


Fig. 12 Density reduction rate as caused by rupture of saturated steam pipe at 50% load



*Fig. 13 Density reduction rate as caused by simultaneous rupture of the superheated and saturated steam pipes and influenced by the inlet volume*

$$\left(\frac{d\rho}{dt}\right)_m$$

$$\left[\frac{\text{kg/m}^3}{\text{sec}}\right]$$

$$V_i = 100 \text{ m}^3$$

$$V_h = 25 \text{ m}^3$$

$$V_e = 200 \text{ m}^3$$

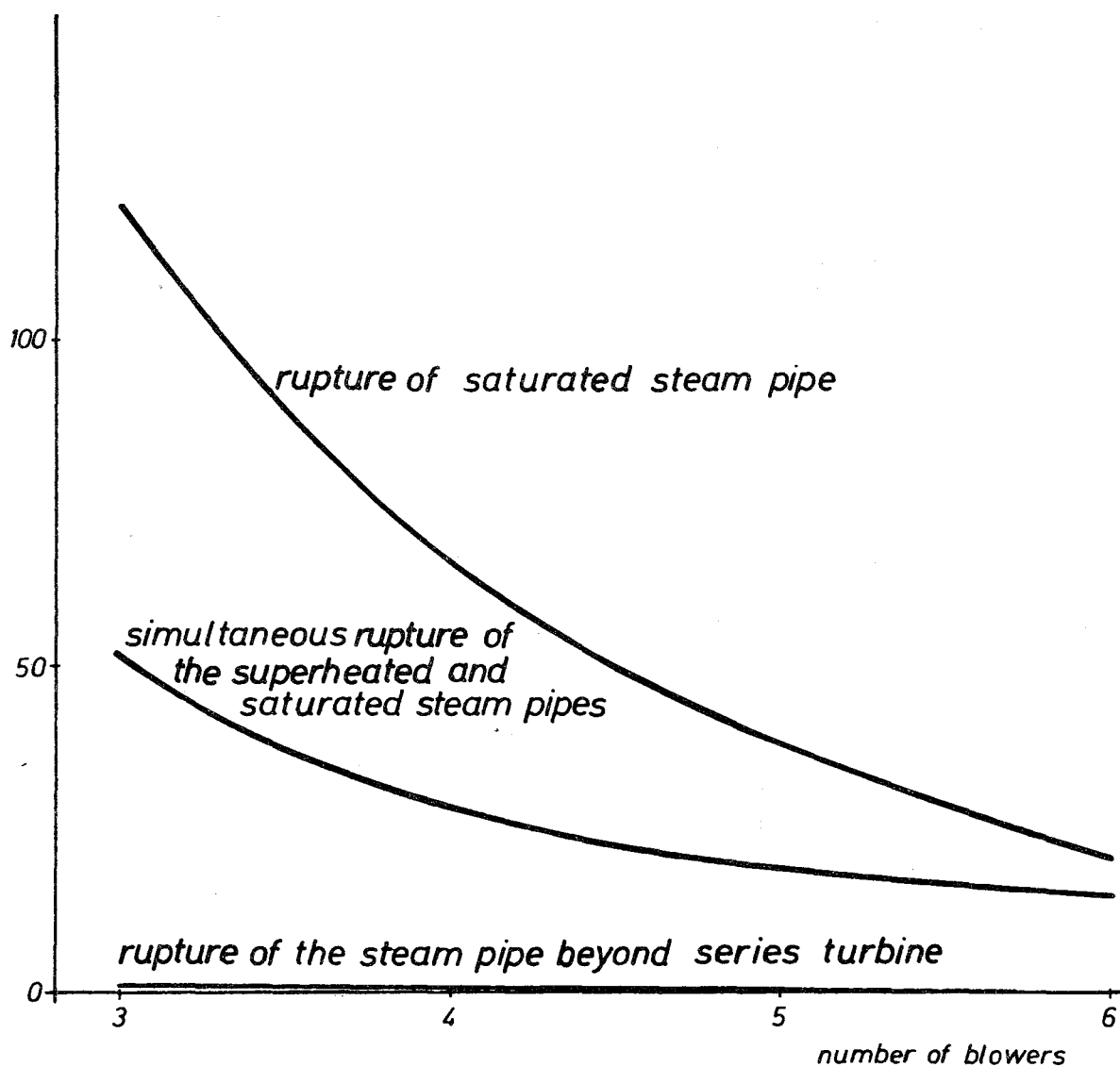
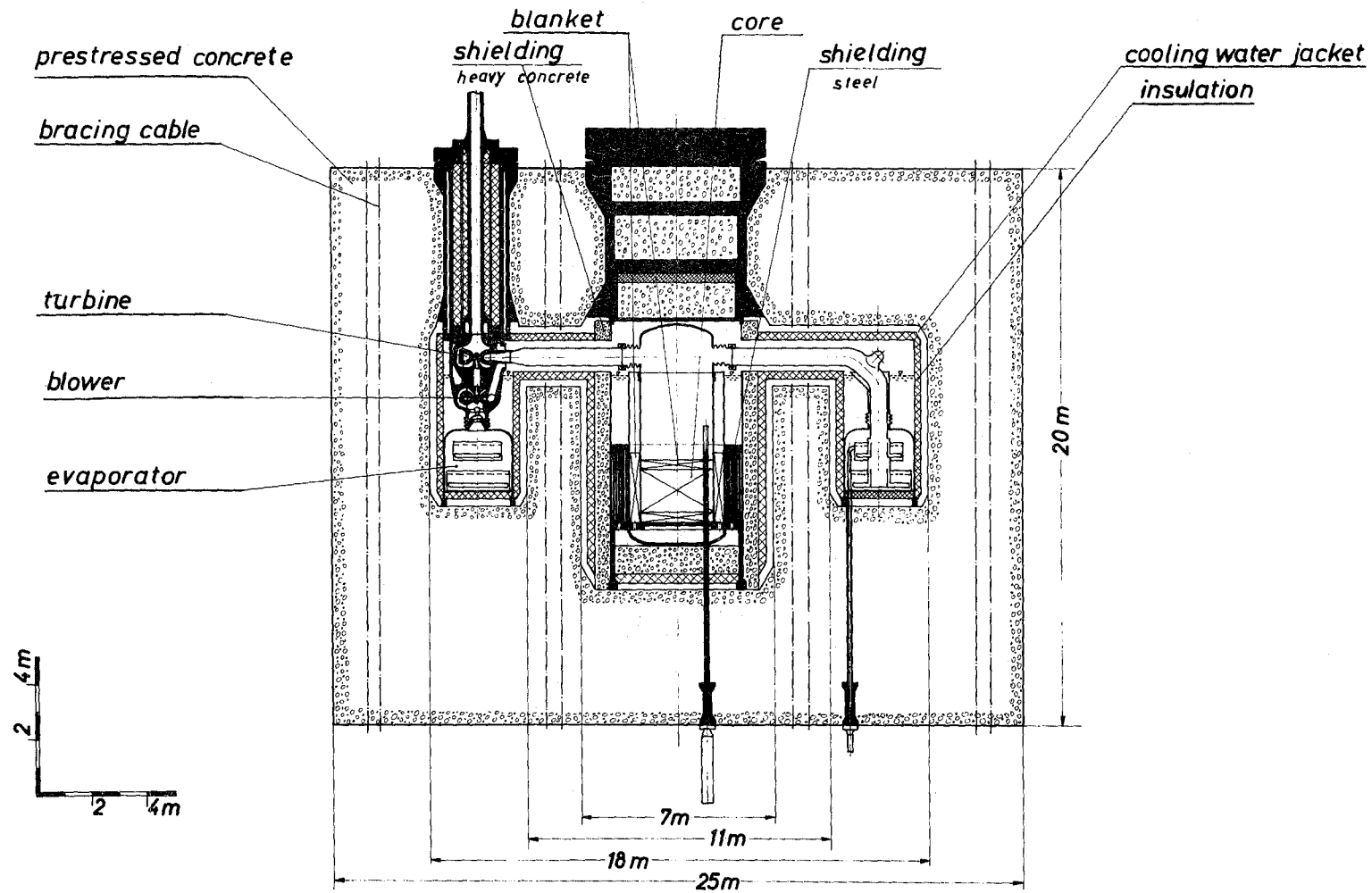
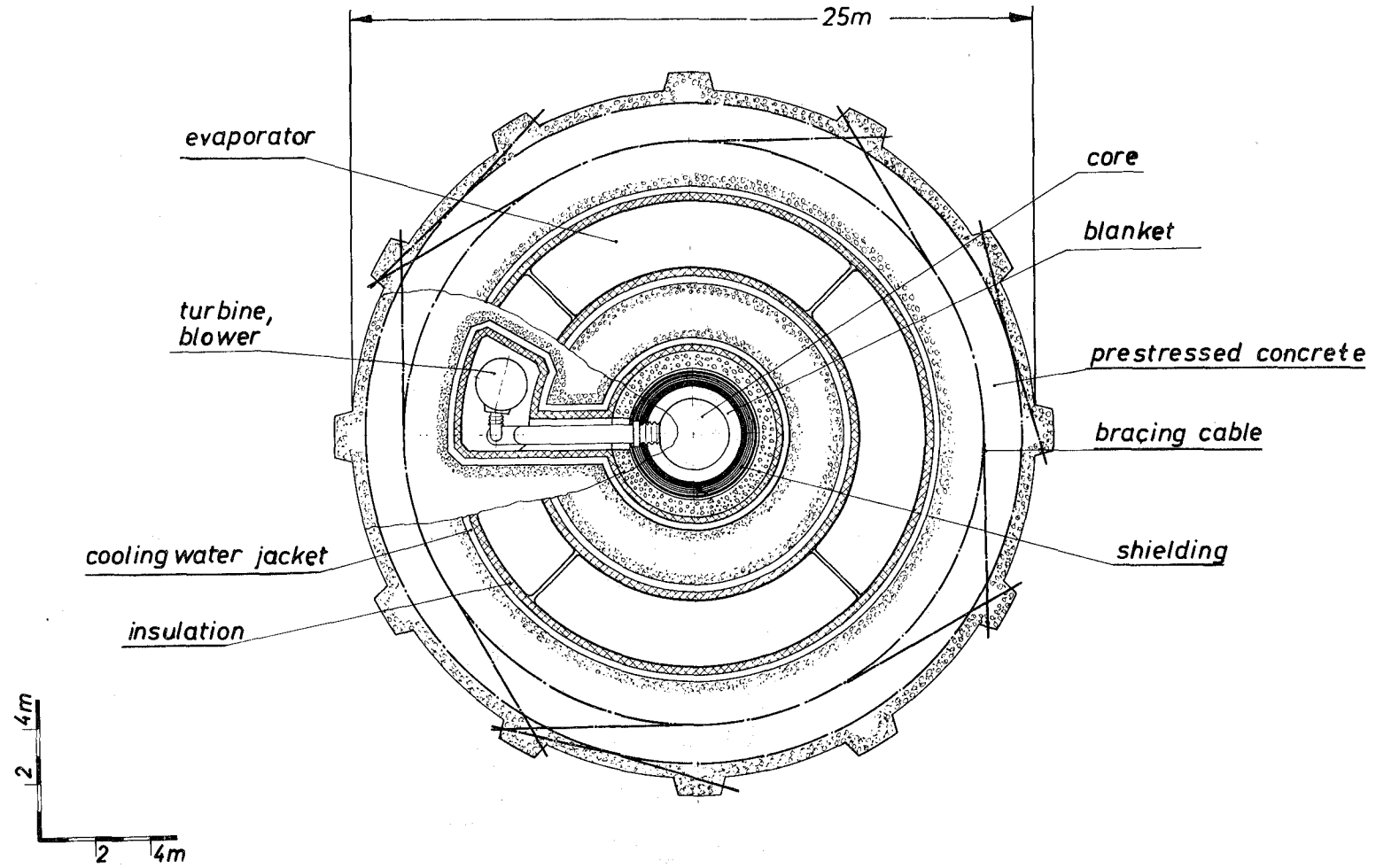


Fig.14 Density reduction rate as caused by various pipe ruptures and influenced by the number of blowers



**Fig. 15** Arrangement of an integrated cooling cycle for a 1000 MW(e) steam cooled fast breeder reactor (longitudinal cross section)



**Fig. 16** Arrangement of an integrated cooling cycle for a 1000 MW(e) steam cooled fast breeder reactor (horizontal cross section)



location of volumes		realized volumes [m <sup>3</sup> ]	required volumes for inherent stability [m <sup>3</sup> ]	
			favourable value	upper limit
water reservoir around the core	$V_w$	60	50	200
water in the evaporators	$V_{ew}$	60	50	100
steam in the evaporators	$V_{es}$	200	100	300
saturated steam header	$V_s$	60	50	200
superheated steam header	$V_h$	40	30	120

Fig.17 Volumes as realized by an integrated cooling cycle for a 1000 MW(e) steam cooled fast breeder reactor

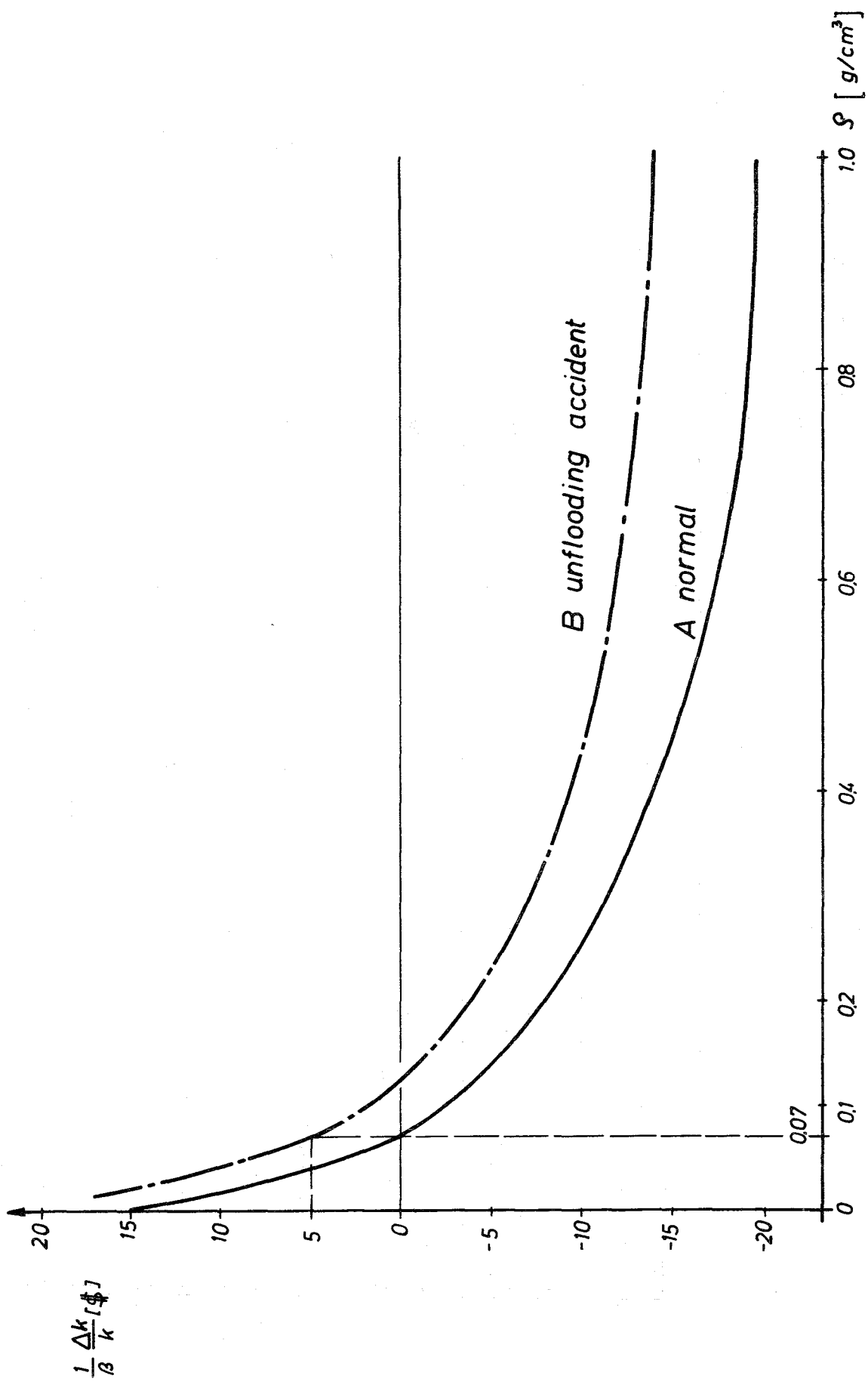
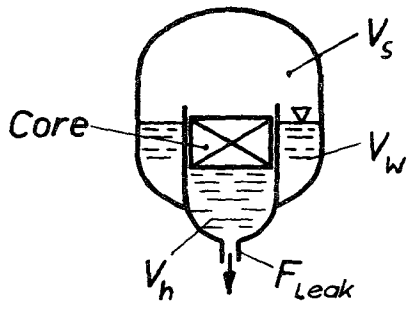
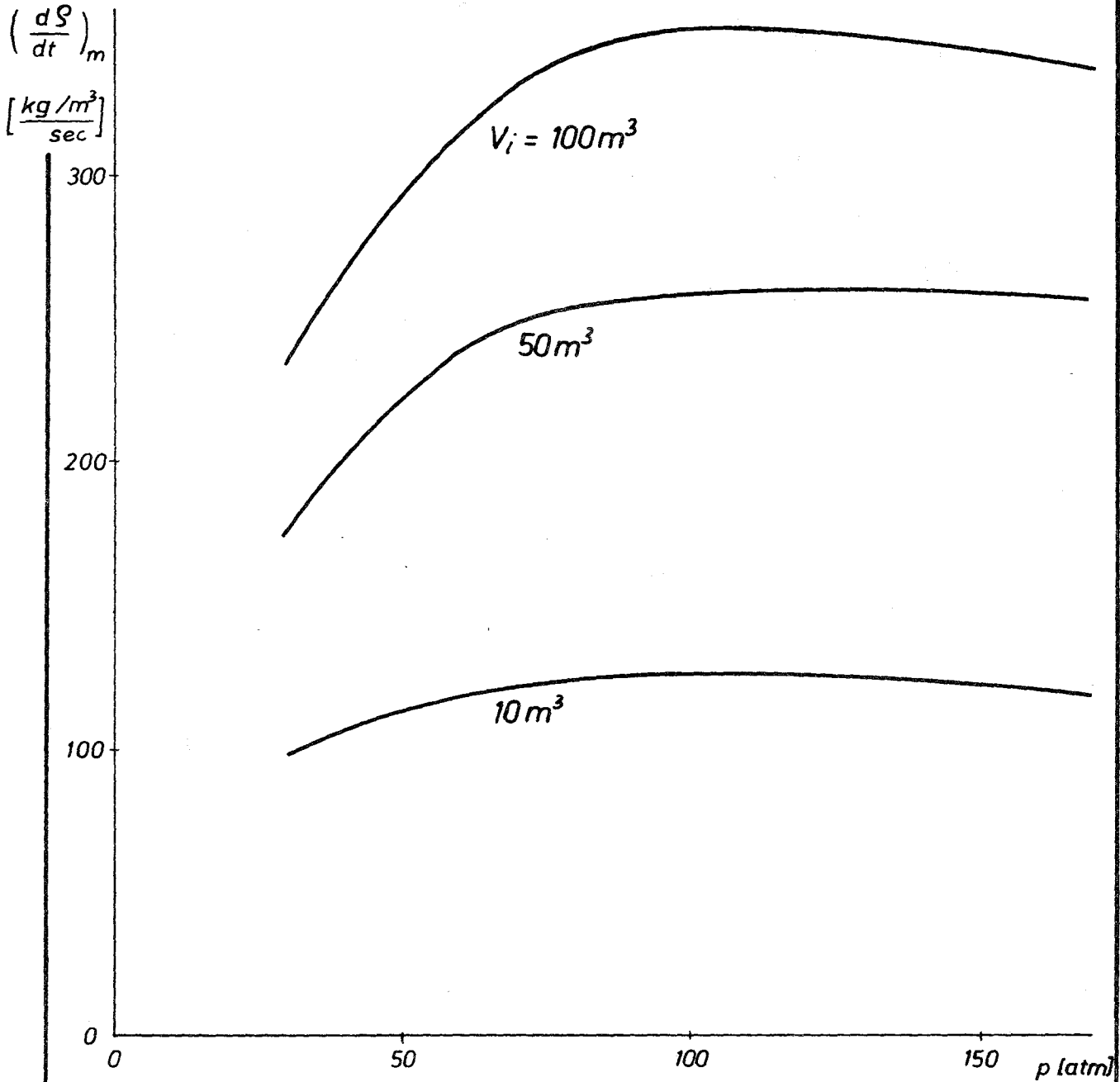


Fig. 18 Reactivity versus steam density



$$V_i = V_w + \frac{V_s}{R}$$



**Fig. 19** Density reduction rate of unloading accident as influenced by the pressure

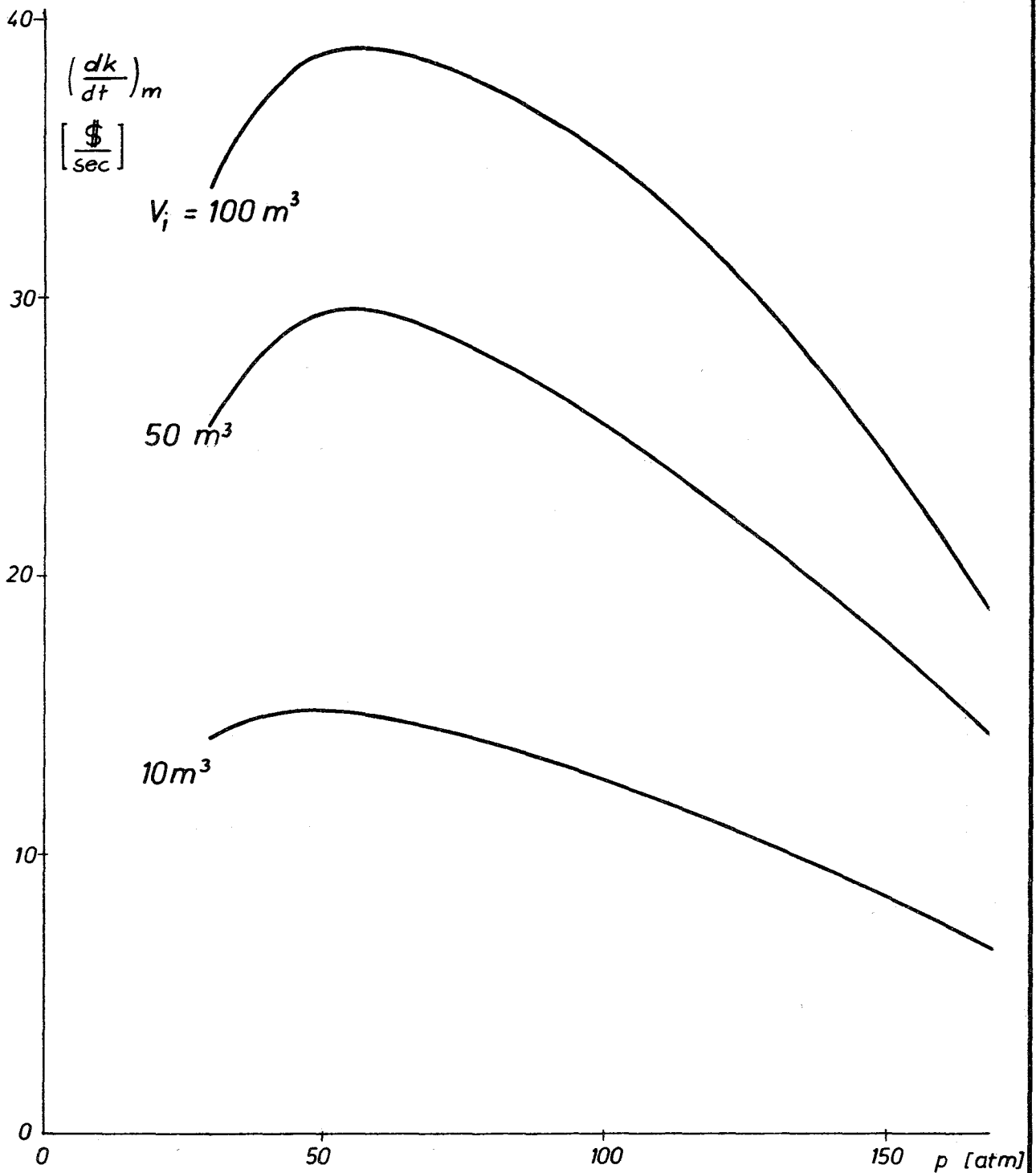


Fig. 20 Reactivity rate of unflooding accident as influenced by the pressure

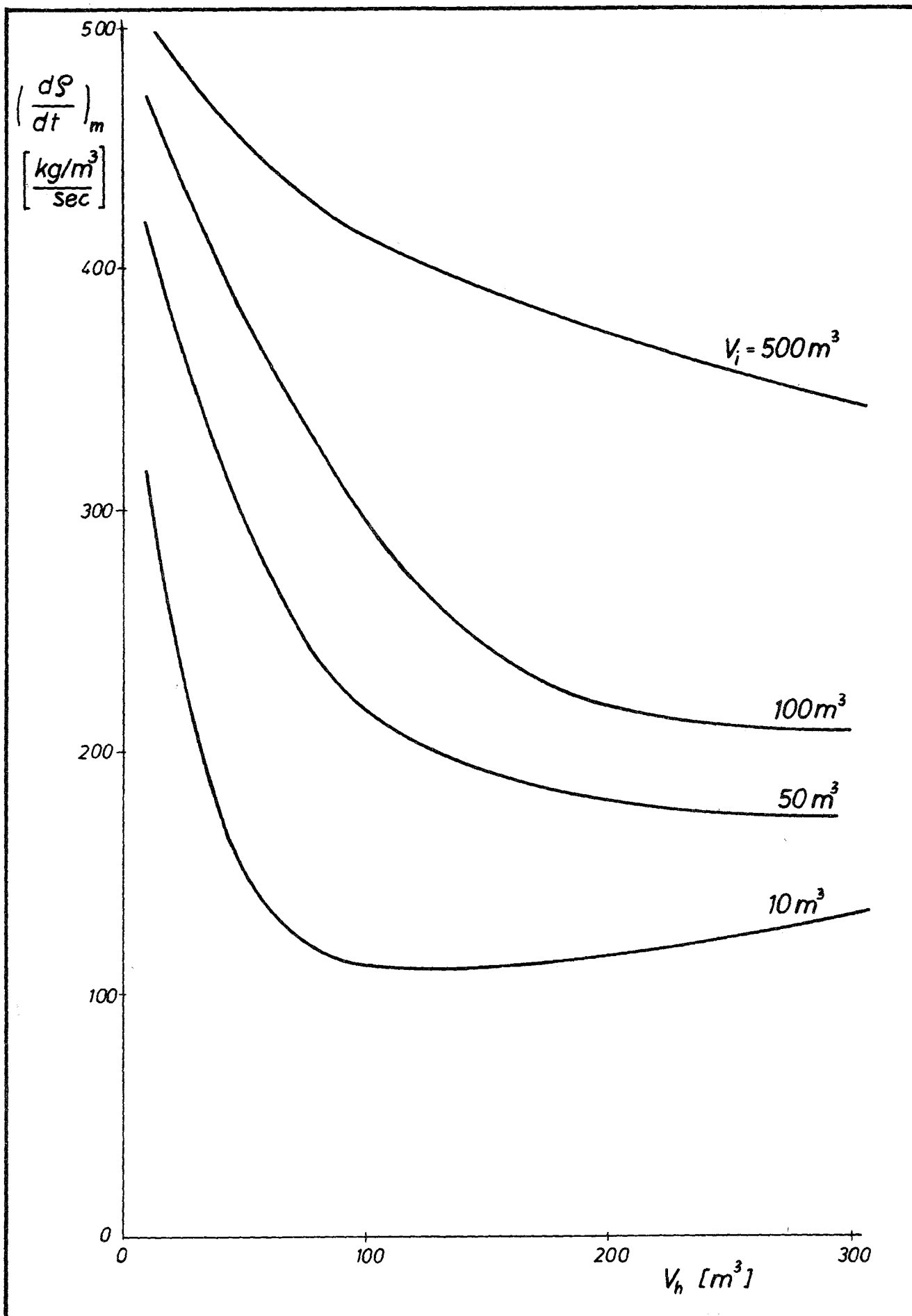


Fig.21 Density reduction rate of unflooding accident as influenced by the volumes